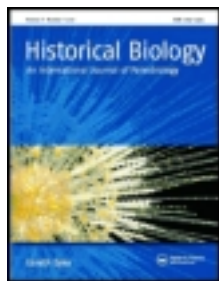


This article was downloaded by: [University of Antioquia]

On: 08 January 2014, At: 08:23

Publisher: Taylor & Francis

Informa Ltd Registered in England and Wales Registered Number: 1072954 Registered office: Mortimer House, 37-41 Mortimer Street, London W1T 3JH, UK



## Historical Biology: An International Journal of Paleobiology

Publication details, including instructions for authors and subscription information:

<http://www.tandfonline.com/loi/ghbi20>

### Osteology and phylogenetic relationships of *Tyrannotitan chubutensis* Novas, de Valais, Vickers-Rich and Rich, 2005 (Theropoda: Carcharodontosauridae) from the Lower Cretaceous of Patagonia, Argentina

Juan Ignacio Canale<sup>ab</sup>, Fernando Emilio Novas<sup>ac</sup> & Diego Pol<sup>ad</sup>

<sup>a</sup> CONICET: Consejo Nacional de Investigaciones Científicas y Técnicas, Argentina

<sup>b</sup> Museo Municipal 'Ernesto Bachmann', Dr. Natali S/N Villa El Chocón (8311), Neuquén, Argentina

<sup>c</sup> Laboratorio de Anatomía Comparada y Evolución de los Vertebrados, Museo Argentino de Ciencias Naturales 'Bernardino Rivadavia', Av. Ángel Gallardo 470 (C1405DJR), Buenos Aires, Argentina

<sup>d</sup> Museo Paleontológico 'Egidio Feruglio', Fontana 140, 9100, Trelew Chubut Argentina

Published online: 08 Jan 2014.

To cite this article: Juan Ignacio Canale, Fernando Emilio Novas & Diego Pol, Historical Biology (2014): Osteology and phylogenetic relationships of *Tyrannotitan chubutensis* Novas, de Valais, Vickers-Rich and Rich, 2005 (Theropoda: Carcharodontosauridae) from the Lower Cretaceous of Patagonia, Argentina, Historical Biology: An International Journal of Paleobiology

To link to this article: <http://dx.doi.org/10.1080/08912963.2013.861830>

PLEASE SCROLL DOWN FOR ARTICLE

Taylor & Francis makes every effort to ensure the accuracy of all the information (the "Content") contained in the publications on our platform. However, Taylor & Francis, our agents, and our licensors make no representations or warranties whatsoever as to the accuracy, completeness, or suitability for any purpose of the Content. Any opinions and views expressed in this publication are the opinions and views of the authors, and are not the views of or endorsed by Taylor & Francis. The accuracy of the Content should not be relied upon and should be independently verified with primary sources of information. Taylor and Francis shall not be liable for any losses, actions, claims, proceedings, demands, costs, expenses, damages, and other liabilities whatsoever or howsoever caused arising directly or indirectly in connection with, in relation to or arising out of the use of the Content.

This article may be used for research, teaching, and private study purposes. Any substantial or systematic reproduction, redistribution, reselling, loan, sub-licensing, systematic supply, or distribution in any form to anyone is expressly forbidden. Terms & Conditions of access and use can be found at <http://www.tandfonline.com/page/terms-and-conditions>

# Osteology and phylogenetic relationships of *Tyrannotitan chubutensis* Novas, de Valais, Vickers-Rich and Rich, 2005 (Theropoda: Carcharodontosauridae) from the Lower Cretaceous of Patagonia, Argentina

Juan Ignacio Canale<sup>a,b\*</sup>, Fernando Emilio Novas<sup>a,c,1</sup> and Diego Pol<sup>a,d,2</sup>

<sup>a</sup>CONICET: Consejo Nacional de Investigaciones Científicas y Técnicas, Argentina; <sup>b</sup>Museo Municipal 'Ernesto Bachmann', Dr. Natali S/N Villa El Chocón (8311), Neuquén, Argentina; <sup>c</sup>Laboratorio de Anatomía Comparada y Evolución de los Vertebrados, Museo Argentino de Ciencias Naturales 'Bernardino Rivadavia', Av. Ángel Gallardo 470 (C1405DJR), Buenos Aires, Argentina; <sup>d</sup>Museo Paleontológico 'Egidio Feruglio', Fontana 140, 9100 Trelew, Chubut, Argentina

(Received 1 October 2013; accepted 30 October 2013)

The theropod clade Carcharodontosauridae is a broadly distributed group of large allosauroid theropods. The carcharodontosaurids recorded in the Albian–Cenomanian of Gondwana are the youngest and most derived members of this clade. *Tyrannotitan chubutensis*, from the Cerro Castaño Member of Cerro Barcino Formation (Albian; Chubut Group), Central Patagonia, Argentina, is of prime interest among Gondwanan carcharodontosaurids as it represents the oldest record of the group. Here we offer a detailed osteological comparative description of the holotype and paratype of *Tyrannotitan chubutensis* together with a new diagnosis of the species. The new information results in a better understanding of this taxon and Carcharodontosauridae. Furthermore, a comparative study of the anatomy of the pectoral girdle of *Giganotosaurus* is reinterpreted as very similar to that of *Tyrannotitan* and *Mapusaurus*. We also present a phylogenetic analysis of Carcharodontosauridae that recovers *Tyrannotitan* as a derived carcharodontosaurid, being the sister group of the clade formed by *Giganotosaurus* and *Mapusaurus*, all nested in the clade Giganotosaurini.

**Keywords:** Theropoda; Carcharodontosauridae; *Tyrannotitan*; Patagonia; Argentina

## 1. Introduction

Allosauroid theropods, and particularly carcharodontosaurids, have been the focus of recent research (Novas et al. 2005; Coria and Currie 2006; Brusatte and Sereno 2008; Sereno and Brusatte 2008; Brusatte et al. 2009; Ortega et al. 2010). Although Carcharodontosauridae was formerly interpreted as a group of gigantic Gondwanan predatory dinosaurs, this clade is now known to be present in both the southern and northern hemispheres (Brusatte et al. 2009, 2012; Ortega et al. 2010). New carcharodontosaurid taxa have been recovered from different localities in the northern hemisphere, such as Spain (Ortega et al. 2010) and China (Brusatte et al. 2009; Brusatte et al. 2012), distant from the 'classic' localities in South America and Africa (Stromer 1931; Coria and Salgado 1995; Sereno et al. 1996; Sereno and Brusatte 2008). Recently, Benson et al. (2010) considered that some 'problematic' carnivorous dinosaurs from southern continents, including *Megaraptor*, *Orkoraptor*, *Australovenator* and *Aerosteon* (all grouped in a clade called Megaraptora), with the European form *Neovenator* as their sister group, constitute a monophyletic clade that conform the sister group of Carcharodontosauridae: the Neovenatoridae. In this way, these authors established the new clade Carcharodontosauria, which includes Neovenatoridae and Carcharodontosauridae. This

proposal was recently challenged by Novas et al., which considered Megaraptora as more closely related to tyrannosauroid coelurosaur theropods (Novas et al. 2013) than to carcharodontosaurids.

The phylogenetic relationships within carcharodontosaurids have been highly debated, in spite of the few detailed anatomical descriptions available for most carcharodontosaurids (Coria and Currie 2006; Brusatte and Sereno 2007; Eddy and Clarke 2011). Therefore, the description in detail of carcharodontosaurid remains is necessary in order to understand the basic osteology, as well as, the phylogenetic relationships of this group.

The aim of this paper was to provide a detailed osteological description of *Tyrannotitan chubutensis* Novas, de Valais, Rich and Rich, 2005, including a new and revised diagnosis of the genus and species. We also present and discuss a phylogenetic analysis of carcharodontosaurids, including the anatomical information obtained from the study of both specimens of *Tyrannotitan* and new data of other carcharodontosaurid taxa.

## 2. Institutional abbreviations

BYU-VP: Brigham Young University, Vertebrate Paleontology collection, Provo, Utah, USA MACN-CH: Museo

\*Corresponding author. Email: [juanignaciocanale@hotmail.com](mailto:juanignaciocanale@hotmail.com)

Argentino de Ciencias Naturales ‘Bernardino Rivadavia’, colección Chubut, Buenos Aires, Argentina; MCF-PVPH: Museo Municipal ‘Carmen Funes’, Plaza Huincul, Provincia de Neuquén, República Argentina; MMCh-PV: Museo Paleontológico ‘Ernesto Bachmann’, colección Paleontología Vertebrados, Villa El Chocón, Provincia de Neuquén, Argentina; MNN IGU: Musée National du Niger, Iguidi collection. Niger; MPEF-PV: Museo Paleontológico ‘Egidio Feruglio’, colección Paleontología Vertebrados, Trelew, Provincia de Chubut, Argentina; MUCPV: Museo de la Universidad del Comahue, Ciudad de Neuquén, Provincia de Neuquén, Argentina; MUCPV-Ch: Museo de la Universidad del Comahue, Colección Chocón, Villa El Chocón, Provincia de Neuquén, República Argentina; NCSM: North Carolina State Museum of Natural Sciences, Raleigh, North Carolina, USA; SGM-Din: Ministère de l’Energie et des Mines, dinosaur collection, Rabat, Morocco; UMNH-VP: Utah Museum of Natural History, Vertebrate Paleontology collection, Salt Lake City, Utah, USA.

### 3. Anatomical abbreviations

abr, articular brace; ac, acetabulum; acd, anterior centrodiapophyseal lamina; af, antorbital fossa; al, accessory lamina; ap, acromion process; avp, anteroventral process; bict, biceps tubercle; cf, coracoid foramen; cfu, collateral furrow; cp, collateral pit; cprf, centroprezygapophyseal fossa; cpvl, centroprezygapophyseal lamina; ctf, crista tibiofibularis; dc, distal carina; df, dorsal fossa; dia, diapophysis; dpc, deltopectoral crest; ep, epiphysis; f, foramen; ff, fibular fossa; fh, femoral head; flf, flexor fossa; foc, facet for occipital condyle; ft, fourth trochanter; gf, glenoid fossa; haya, hypantrum; hys, hyosphene; idp, interdental plates; ift, iliofibularis tubercle; il, ilium; ilped, iliac peduncle; iprf, infraprezygapophyseal fossa; jaf, articular facet for jugal; jpr, jugal pneumatic recess; lc, lateral condyle; lf, lateral fossa; lmf, lateromedial furrow; ls, ligament scar; lt, lesser trochanter; mc, mesial carina; mco, mesial condyle; mf, Meckelian fossa; mfp, medial fibular pocket; mg, Meckelian groove; nc, neural canal; nvf, neurovascular foramen; nvg, neurovascular groove; on, obturator notch; op, obturator process; paf, articular facet for postorbital; pcd, posterior centrodiapophyseal lamina; pec, prezygoepiphysal crest; pf, pubic foramen; pl, pleurocoel; po, pneumatic opening; pvp, posteroventral process; poz, postzygapophysis; pp, parapophysis; ppdl, paradiapophyseal lamina; pped, pubic peduncle; prz, prezygapophysis; ps, pubic symphysis; pvp, posteroventral process; r, ridge; rcl, ridge for cruciate ligaments; spol, spinopostzygapophyseal lamina; spof, spinopostzygapophyseal fossa; sprl, spinoprezygapophyseal lamina; sprf, spinoprezygapophyseal fossa; tp, transverse process; tub, tuberosity; vf, ventral fossa.

### 4. Systematic paleontology

**Dinosauria** Owen, 1842

**Saurischia** Seeley, 1888

**Theropoda** Marsh, 1881

**Allosauroidea** Marsh, 1878

**Carcharodontosauridae** Stromer, 1931

**Carcharodontosaurinae** Stromer, 1931 (*nomen translatum* Brusatte and Sereno, 2008)

**Giganotosaurini** Coria and Currie, 2006 (*nomen translatum* Brusatte and Sereno, 2008)

***Tyrannotitan chubutensis*** Novas, de Valais, Vickers-Rich and Rich, 2005

#### 4.1 Holotype

MPEF-PV 1156: Partially articulated skeleton, composed of right dentary with two complete teeth, left dentary, articulated dorsal vertebrae 2nd to 7th, 8th? to 11th? dorsals, 14th? dorsal, 1st? sacral vertebra, anterior caudal vertebra, left scapula and coracoid, right humerus, both radii, fragments of left ilium, both ischia, both pubis, both femora, left fibula, six haemal arches and fragments of gastralia.

#### 4.2 Paratype

MPEF-PV 1157: Composed by right jugal, right quadratojugal, right dentary, two isolated teeth, 7th cervical vertebra, 1st dorsal vertebra, 4th dorsal, 6th to 8th dorsals, 12th to 14th dorsals, isolated neural spine of a posterior dorsal vertebra, incomplete sacrum, distal caudal vertebra, proximal fragment of dorsal rib, right dorsal rib 14, haemal arch, right femur, left metatarsal II and left pedal phalanges II-2, II-3, IV-2, IV-3. The specimen was found 1 km from the holotype material.

#### 4.3 Referred material

MPEF-PV 10821: 19 isolated teeth found in this locality, which are housed at the MPEF collections but have not been assigned to the holotype or paratype. Only two isolated teeth have been catalogued as part of the paratype (MPEF-PV 1157; see above).

#### 4.4 Locality and horizon

‘La Juanita’ farm, 28 km north-west of Paso de Indios town, Chubut Province, Argentina (Figure 1). Precise GPS data of the fossiliferous localities are deposited at the MPEF collection and available upon request. Cerro Castaño Member, Cerro Barcino Formation, Albian (Musacchio and Chebli 1975; Codignotto et al. 1978; Rich et al. 2000; Marveggio and Llorens 2013).

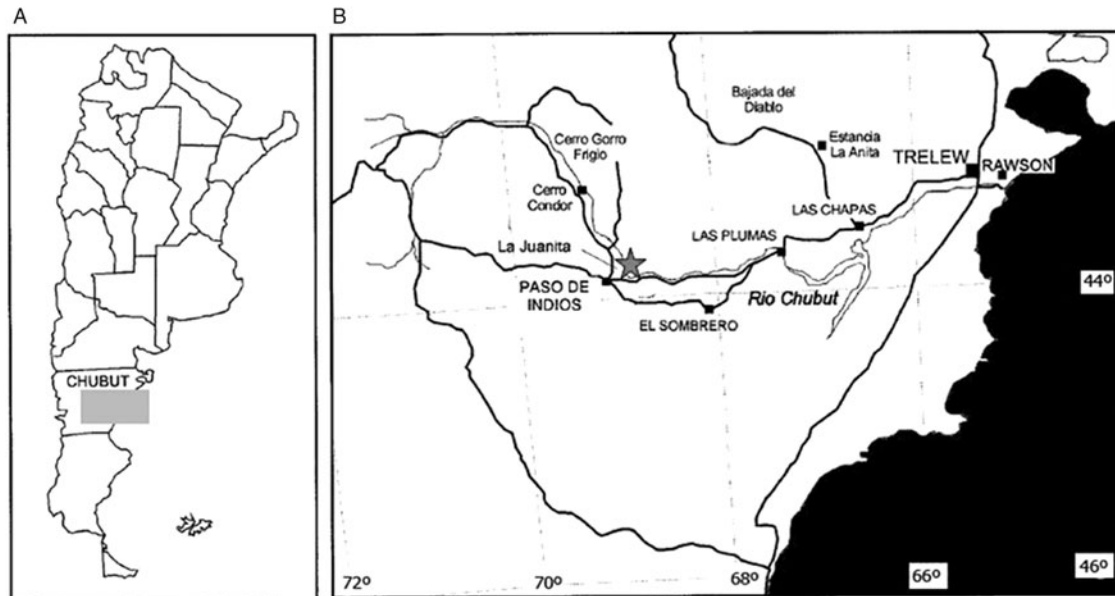


Figure 1. *Tyrannotitan chubutensis* (Novas et al. 2005) locality map: (A) Argentina and (B) detail of Chubut province with the *Tyrannotitan* locality indicated by a star.

Cerro Barcino Formation is the upper unit of the Chubut Group and its age has been regarded as Hauterivian to Senonian (Campanian?) in age (Page et al. 1999), and is subdivided into several members. The basalmost member is Puesto La Paloma and is characterised by pyroclastic and fluvial sediments, with dunes intercalated deposited under arid conditions. This unit contains chelid and meiolaniform turtles (Gaffney et al. 2007; de la Fuente et al. 2011; Sterli et al. 2013), as well as abelisaurid theropod and titanosauriform sauropod dinosaurs (Rich et al. 2000; Rauhut et al. 2003). Overlying La Paloma Member is the Cerro Castaño Member, formed mainly by fluvial sediments. Sedimentological evidence indicates that during deposition of the Cerro Castaño Member, a return to wetter conditions occurred over the previous unit. Apart from *Tyrannotitan* (Novas et al. 2005), this member has provided a variety of vertebrate remains, including crocodiles (Leardi and Pol 2009), sphenodontians (Apesteguía and Carballido in press), sauropod eggs (Aragañaz et al. 2013) and possibly the ceratosaur theropod *Genyodectes serus* (Rauhut et al. 2003; Rauhut 2004). Cerro Barcino Formation culminates with Bayo Overo Member, in which the titanosauriform sauropod *Chubutisaurus insignis* was found (Del Corro 1975; Carballido et al. 2011).

#### 4.5 Emended diagnosis

A carcharodontosaurid theropod diagnosed by the following autapomorphic characters: teeth with bilobated denticles in the mesial carinae; dentary with an

anteroventrally-posterodorsally symphyseal margin in lateral view; second and third dorsal vertebrae with well-developed accessory lamina connecting anterior and posterior centrodiapophyseal laminae; fibular fossa extended over the proximal end of the crista tibiofibularis in the femoral shaft; proximomedial fossa of the fibula with posteriorly projected anterior border. Modified from Novas et al. (2005) (see Section 6).

## 5. Description

### 5.1 Jugal

The right jugal of the paratype (MPEF-PV 1157) is well preserved, but lacks a fragment of its anterior portion, the surface for the maxilla/lacrimal contact surface and the quadratojugal processes (Figures 2 and 7).

The jugal is a transversely flattened bone that has an anterior projection for articulation with the maxilla, a dorsal process to contact the postorbital and a double posterior projection for articulation with the quadratojugal. In lateral view the ventral margin of the bone is straight to slightly convex (Figure 2), as in *Carcharodontosaurus saharicus* (SGM-Din 1) and *Mapusaurus* (MCF-PVPH 108,167), but differing from that of *Allosaurus* (UMNH-VP 9085, UMNH-VP 9086) where the ventral margin is sigmoid in lateral view, with a strong convexity ventral to the level of the postorbital process. In ventral view, the jugal has a sigmoidal shape, with the anterior region laterally concave and the posterior portion laterally convex.

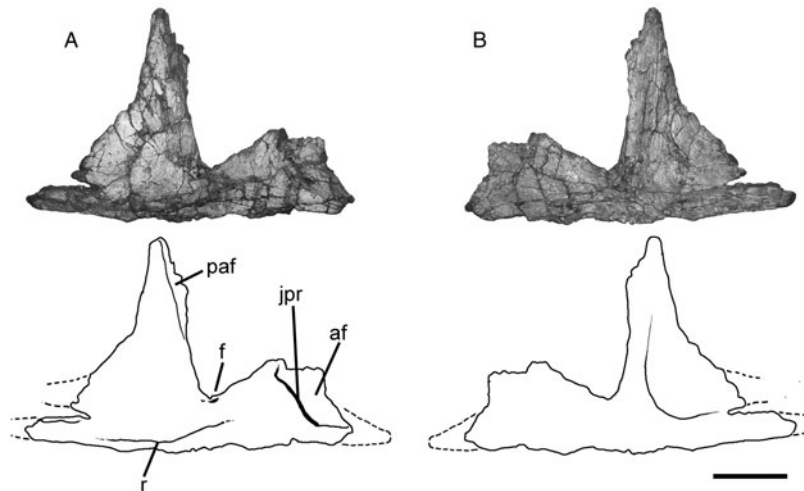


Figure 2. *Tyrannotitan chubutensis* right jugal (MPEF-PV 1157) photographs and line drawings in (A) lateral view and (B) medial view. Note: Scale bar is 10 cm; see text for abbreviations.

The anterior end of the jugal is thin and laminar, incompletely preserved in some areas, and bears on its lateral surface the posteroventral corner of the antorbital fossa (Figure 2(A)). The edge of this fossa is curved, with a similar position and morphology to that of *Mapusaurus* (MCF-PVPH 108.167) and *Allosaurus* (Madsen 1976). A large jugal pneumatic recess is also present, and is as expanded as in *Mapusaurus* (MCF-PVPH 108.167) and *Acrocanthosaurus* (NCSM 14345).

A prominent horizontal ridge runs along most of the lateral surface of the jugal, which extends from the notch between the two quadratojugal processes towards few centimetres anteriorly to the anterior margin of the postorbital process. This crest, also present in *Mapusaurus* (MCF-PVPH 108.167), was probably an insertion area for the *m. pterygoideus ventralis* (Holliday 2009).

Ventrally to the ventral edge of the orbital margin, the jugal is pierced by a foramen of about 1 cm in diameter, which penetrates into the bone internal structure (Figure 2 (A)). Posteriorly to this foramen, there is a much smaller and rounded blind depression.

The postorbital process of jugal is triangular in lateral view, with the anterior margin nearly straight and subvertically oriented. In cross section this process has a rounded and robust anterior end and tapers posteriorly becoming a thin lamina at its posterior margin. The base of this process is anteroposteriorly long, as in *Mapusaurus* (MCF-PVPH 108.167-168), but differing from the condition of *Carcharodontosaurus saharicus* (SGM-Din 1) in which the process is anteroposteriorly short. On the anterior margin the oblique and anterolaterally oriented postorbital facet occupies the dorsal three-quarters of the postorbital process (Figure 2(A)). The laminar posterior margin of the process bears a slight depression, corresponding to the anterior edge of the infratemporal fossa.

The articulation for the quadratojugal is forked into dorsal and ventral quadratojugal processes. Both processes have their posterior end broken, being the ventral process the most completely preserved. The latter is subcircular in cross-section and bears a dorsal concavity. The dorsal process is laminar in cross-section. The posterior region of the jugal of *Tyrannotitan* lacks, both laterally and medially, a third medial process or accessory prong (contra Eddy and Clarke 2011), as was described for *Acrocanthosaurus* (Eddy and Clarke 2011), *Sinraptor* (Currie and Zhao 1993) and *Mapusaurus* (MCF-PVPH 108.168).

### 5.2 Quadratojugal

The right quadratojugal has been preserved in MPEF-PV 1157 (Figures 3 and 7). The jugal process is dorsoventrally high, and becomes narrower towards its anterior end. The squamosal process has a fairly constant anteroposterior width along the dorsoventral axis throughout its entire length. In lateral view, the height of the jugal process is larger than the anteroposterior width of the squamosal process, unlike *Allosaurus* (UMNH-VP 8944, UMNH-VP 8946) and *Acrocanthosaurus* (NCSM 14345) in which an inverse relationship is present. In the posteroventral corner, this bone has a posterior process similar to that of other theropods. In medial view, a shallow depression is present at the dorsal sector of the jugal process. This depression represents the area for the articulation of the posterodorsal process of the jugal.

### 5.3 Dentary

The three available dentaries are preserved in a fairly good condition, lacking only the posteriormost portion that

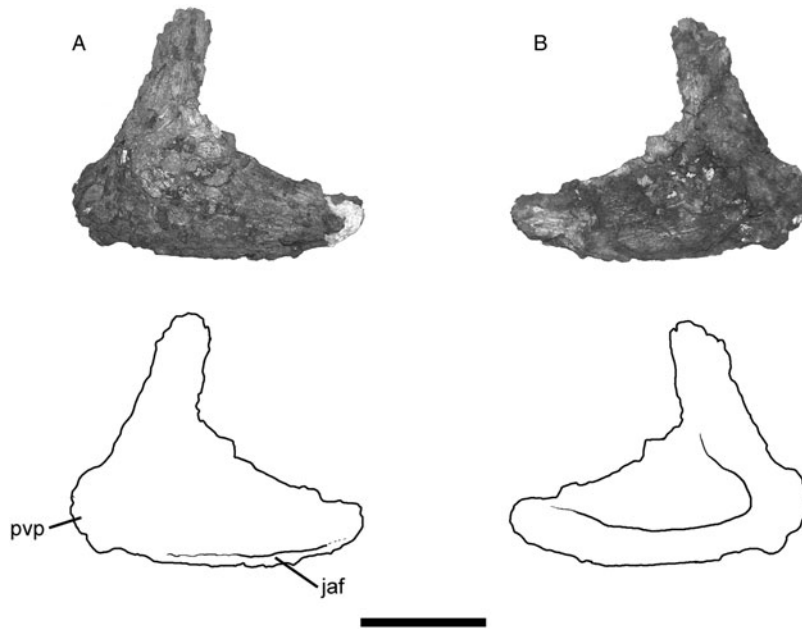


Figure 3. *Tyrannotitan chubutensis* right quadratojugal (MPEF-PV 1157) photographs and line drawings in (A) lateral view and (B) medial view. Note: Scale bar is 10 cm; see text for abbreviations.

contacts the postdentary bones. The following description is based on the three elements.

In dorsal view, the dentary is transversely compressed, and slightly widens anteriorly towards the symphyseal area (Figure 4(C)). This feature is reminiscent to that of other allosauroids, such as in *Giganotosaurus* (MUCPV-Ch 1), *Acrocanthosaurus* (NCSM 14345), *Allosaurus* (UMNH-VP 9351), but differs from abelisaurids (e.g. *Carnotaurus* (MACN-CH 894), *Ekrixinatosaurus* (MUCPV-294), *Skorpiovenator* (MMCh-PV 48) in which the dentary has a constant transverse width

throughout its entire length. The dentary of *Tyrannotitan* is nearly straight along most of its length, showing a slight medial curvature near its anterior end, at the level of the anterior edge of the third alveolus. In *Giganotosaurus* (MUCPV-Ch 1, MUCPV 95), the medial curvature of the anterior region is more marked and starts more posteriorly, approximately at the anterior border of the sixth alveolus, whereas in *Acrocanthosaurus* (NCSM 14345), the dentary is straight and in *Allosaurus* (UMNH-VP 9351) the dentary is gently curved medially along its entire length. In lateral view, the dentary is posteriorly high and

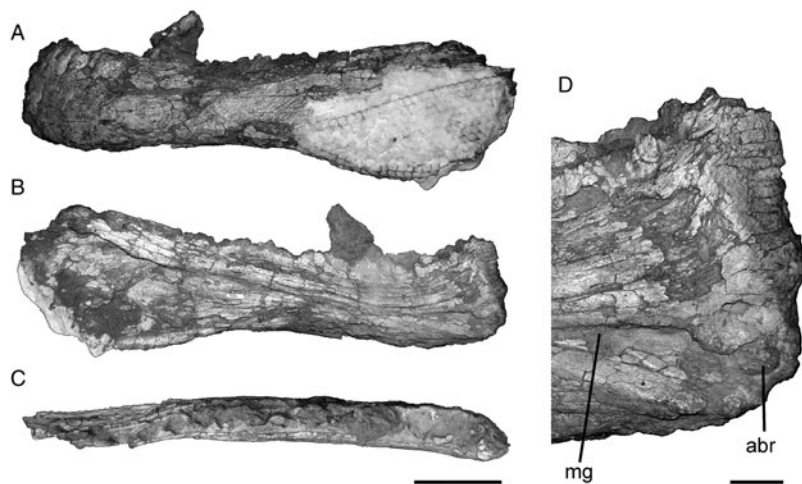


Figure 4. *Tyrannotitan chubutensis* left dentary (MPEF-PV 1156) photographs in (A) lateral view, (B) medial view, (C) dorsal view and (D) detail of the symphysis in medial view. Note: Scale bar is 10 cm in A–C and 2 cm in D; see text for abbreviations.

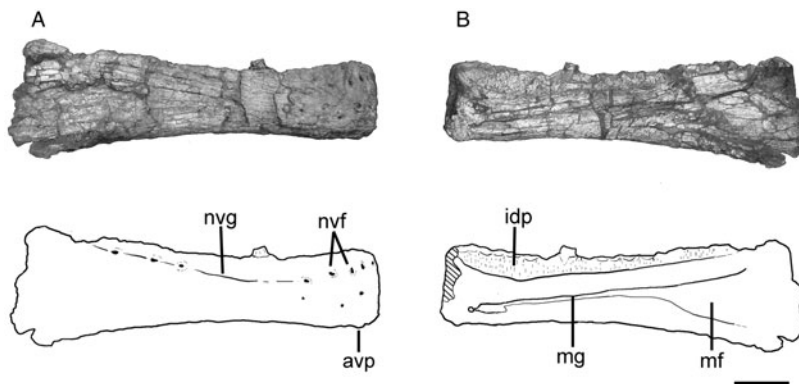


Figure 5. *Tyrannotitan chubutensis* right dentary (MPEF-PV 1157) photographs and line drawings in (A) lateral view and (B) medial view. Note: Scale bar is 10 cm; see text for abbreviations.

progressively tapers anteriorly, but has a dorsoventrally higher anterior end, creating a constriction at its central portion (Figures 4 and 5). This condition is also found in *Giganotosaurus* (MUCPV-Ch 1, MUCPV 95) and *Mapusaurus* (Coria and Currie 2006). In *Acrocanthosaurus* (NCSM 14345), *Allosaurus* (UMNH-VP 9351, UMNH-VP 6476) and the purported carcharodontosaurid *Kelmaysaurus petrolicus* (Brusatte et al. 2012), the dorsoventral dentary height is nearly homogeneous along the entire length of the bone. In *Tyrannotitan* the minimum height of the dentary occurs at the level of the seventh alveolus. The dentary has 15 alveoli, the anteriormost of which is subcircular while all others are ellipsoidal and anteroposteriorly elongated; a morphology that is more pronounced in the posterior alveoli. This contrasts with the condition of *Neovenator* and in most ceratosaurs, in which the alveoli have a subrectangular outline (Serenio et al. 2004; Brusatte et al. 2008; Canale et al. 2009). Anterior alveoli are arranged obliquely to the anteroposterior axis of the dentary. The anterior end of the dentary has a subrectangular contour in lateral view, with the angle between the anterior end of the ventral margin and the symphyseal edge nearly straight. The same subrectangular outline is present in *Giganotosaurus* (MUCPV-Ch 1, MUCPV-95), *Carcharodontosaurus iguidensis* (MNN IGU 5), *Acrocanthosaurus* (NCSM 14345) and in a large specimen of *Allosaurus* (UMNH-VP 6476). However, in *Tyrannotitan* the symphyseal anterior edge is completely vertical with respect to its ventral margin. Moreover, the anteroventral end is more anteriorly projected than the anterodorsal margin, so that the symphyseal edge has a slight anteroventral–posterodorsal orientation, which constitutes an autapomorphy of *Tyrannotitan*. In the anterior end of the ventral margin, there is a ventral process (‘chin’) that is also present in *Giganotosaurus* (MUCPV-Ch 1), *Carcharodontosaurus iguidensis* (MNN IGU 5), *Acrocanthosaurus* (NCSM 14345) and *Mapusaurus* (Coria and Currie 2006). This character is only present

in the dentary of the paratype specimen, and has not been preserved in remaining available dentaries of *Tyrannotitan* (Figure 5).

The anterior margin of the dentary in lateral view bears large and rounded neurovascular foramina. Some of these foramina are located within a longitudinal neurovascular groove, which is located dorsally on the lateral surface of the dentary at its anterior region. This groove bends ventrally at the level of the fourth and fifth alveoli, and more posteriorly it curves dorsally (reaching the alveolar margin at the level of the posteriormost alveolus, (Figure 5 (A)). Therefore, the groove follows a sigmoidal pattern, a feature considered as diagnostic of carcharodontosaurids by Serenio and Brusatte (2008). A similar pattern is present not only in *Carcharodontosaurus iguidensis* (MNN IGU 5), *Giganotosaurus* (MUCPV-Ch 1, MUCPV-95) and *Acrocanthosaurus* (NCSM 14345), but also in *Allosaurus* (UMNH-VP 6476). In *Sinraptor* (Currie and Zhao 1993), the lateral neurovascular groove is relatively straight and is located more dorsally than in the above-mentioned taxa. In *Tyrannotitan*, this lateral neurovascular groove follows the same path and is similarly positioned to a groove located on the medial surface of the dentary, where the ventral ends of the fused dental plates are placed.

The symphyseal area is only well preserved in the right dentary of MPEF-PV 1156. It has two smooth concavities separated by a central ridge at its mid-height. In the ventral concavity there is a small rounded process; also observed in *Carcharodontosaurus iguidensis* (‘articular brace’ sensu Brusatte and Serenio 2007) (Figure 4(D)). The symphyseal surface is set at a wide angle with respect to the medial surface of the dentary, observable in dorsal view. This angle gives a rounded appearance to the symphyseal region of the dentary, but not as rounded as in *Carcharodontosaurus iguidensis* (Brusatte and Serenio 2007). Dorsal to the symphysis a small anterodorsal process is present, as in *Carcharodontosaurus iguidensis* (MNN IGU 5).

Along the medial face of the dentary of *Tyrannotitan*, a thickened bar of bone is present, being more prominent in the anterior sector. This bar forms the dorsal limit of the Meckelian groove and is dorsally limited by a deep neurovascular groove that receives the ventral edge of the dental plates. This medial groove, as mentioned above, follows a similar path as the neurovascular groove of the lateral surface of the dentary. Within this groove, it can be observed in dorsal view two foramina located approximately at the level of the second and third alveoli, as in *Carcharodontosaurus iguidensis* (MNN IGU 5). The dental plates are fused together, and have variable height along the dentary. Its maximum height is located at the level of the central constriction of the dentary, decreasing both anteriorly and posteriorly (Figure 5(B)).

The Meckelian groove in *Tyrannotitan*, as in other carcharodontosaurids, is deep and well defined. As in *Carcharodontosaurus iguidensis* (MNN IGU 5) and *Giganotosaurus* (MUCPV-Ch 1, MUCPV-95), the Meckelian groove in *Tyrannotitan* ends anteriorly at the level of first and second alveoli, whereas in *Acrocanthosaurus* (NCSM 14345) it ends more posteriorly, at the level of third and fourth alveoli. Anteriorly to the Meckelian groove, the dentary bears an anteroposteriorly elongated oval fossa that is preceded anteriorly by a small round foramen (Figure 5(B)). At the level of the dorsoventral constriction of the dentary, the Meckelian groove expands ventrally, forming a broad and subtriangular Meckelian fossa, which receives the anterior process of the splenial. Dorsally to this fossa, the medial surface of the dentary is smooth and flat, as also occurring in *Tyrannosaurus* (Brochu 2003), whereas anteriorly this surface is gently convex. This transition occurs at the level of the 9th to 10th alveoli.

#### 5.4 Teeth

The right dentary of the holotype (MPEF-PV 1156) has the sixth and seventh teeth preserved in their alveoli. The collected materials also include 21 isolated teeth, 2 of which had been referred to the paratype specimen (MPEF-PV 1157). The following description is based on the general characteristics present in all the available teeth.

The teeth are transversely compressed, with a crown base ratio (crown base width/crown base length) that varies between 0.33 and 0.63 (values taken from 13 teeth) (Appendix S4, Table 2). The mesial margin is convex and the distal is in general straight, except for a few teeth that have concave distal margin (Figure 6(D)). In eight of the teeth recovered, the mesial and distal carinae are centrally located, giving the tooth crown a symmetrical cross section. These teeth may have occupied a middle-posterior position in the tooththrow. In the remaining seven teeth that

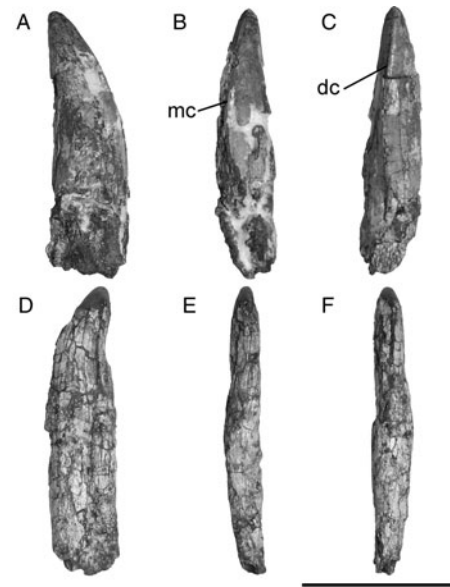


Figure 6. *Tyrannotitan chubutensis* isolated teeth (MPEF-PV 10821) photographs in (A) lateral view, (B) mesial view and (C) distal view of a ‘anterior’ tooth, (D) lateral view, (E) mesial view and (F) distal view of a ‘middle-posterior’ tooth. Note: Scale bar is 5 cm; see text for abbreviations.

have preserved both carinae, the mesial and distal carinae are displaced from the mesiodistal axis, giving the tooth crown an asymmetrical cross section. Probably these teeth were positioned at the anterior region of the tooththrow. The specific position of the isolated teeth (i.e. whether they represent upper or lower teeth, left or right) is difficult to determine, given the variation observed in other theropods. For example, in the abelisaurid *Majungasaurus crenatissimus* (Fanti and Therrien 2007), the anterior teeth have both carinae lingually displaced. However, in the dentary of *Giganotosaurus* (MUCPV-Ch 1), the anteriorly located teeth have their carinae labially displaced, creating a greater convexity on the lingual surface of each tooth. For this reason, in the case of the isolated teeth of *Tyrannotitan*, we have decided not to use the carinae displacement as a parameter to assign the teeth of asymmetric cross section to a particular placement of the tooththrow (left or right side), except for identifying them as positioned anteriorly or middle-posteriorly in the tooththrow. The complete teeth, which have preserved their crown and root, have a sigmoid shape when observed in anterior or posterior view (Figure 6(C)), as in *Giganotosaurus* (MUCPV-Ch 1), *Mapusaurus* (MCF-PVPH 108.9) and *Carcharodontosaurus saharicus* (SGM-Din 1).

The denticles are ‘chisel-like’ (Currie et al. 1990), with poorly developed blood-grooves. In the central sector of both carinae, there are two denticles per mm, as in *Giganotosaurus* (MUCPV-Ch 1), *Carcharodontosaurus saharicus* (SGM-Din 1), *Carcharodontosaurus iguidensis*

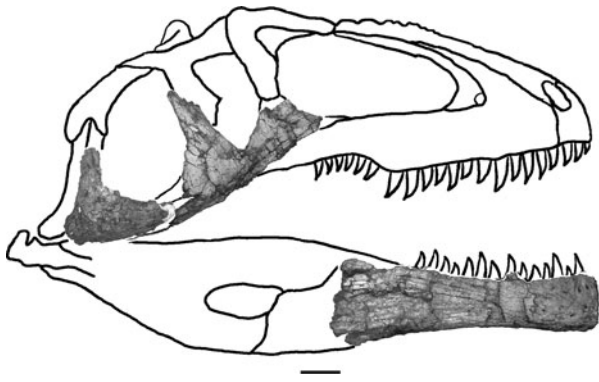


Figure 7. Reconstruction of the lateral side of the skull of *Tyrannotitan chubutensis* based on elements of the paratype (MPEF-PV 1157). Note: Scale bar is 10 cm.

(MNN IGU 6), but differing from *Acrocanthosaurus* (Currie and Carpenter 2000) that has three denticles per mm. Close to the base the denticles are smaller, and the denticle density raises to three per mm. Of the 23 teeth studied, only 5 have preserved a complete mesial carina. Out of those five teeth, only three have bilobulated denticles (the sixth tooth of the right dentary of the holotype plus two isolated teeth). In one of the isolated teeth, the mesial carina extends only over the apical half of the crown. Its ventral half has a smooth and rounded mesial border, lacking a carina or denticles.

At least five teeth have preserved enamel wrinkles, which are present in a wide variety of theropod species (Brusatte et al. 2007; Canale et al. 2009). In *Tyrannotitan chubutensis*, the wrinkles occur variably in each tooth, being located on the mesial carina, on the distal carina or in both carinae. The four teeth preserving the root have a constriction on both the labial and lingual sides, creating an eight-shaped cross section of the root.

### 5.5 Vertebral column

Combining the vertebral elements of both specimens recovered, the available material of *Tyrannotitan* contains representatives of all sections of the vertebral column.

Novas et al. (2005) identified a cervical vertebra of the paratype of *Tyrannotitan* as the ninth cervical. Through comparisons with the cervical series of *Giganotosaurus* (MUCPV-Ch 1), this element is reinterpreted here as the seventh cervical vertebra, given the presence of characters such as a marked opisthocoely of the centrum, a transverse process directed more ventrally than laterally and a neural arch anteroposteriorly extended. Novas et al. (2005) also identified a sequence of articulated vertebrae of the holotype (MPEF-PV 1156), exposed only on its right lateral side, as the segment of third to eighth dorsals. Here, this series is reinterpreted as the sequence of second to seventh dorsals, based on comparison of the neural arch of the first of these articulated elements with the dorsal series of *Allosaurus* (Madsen 1976). The transverse process of this neural arch is laterally directed, making its dorsal surface visible in lateral view. This is consistent with the morphology of the second dorsal of *Allosaurus* (Madsen 1976), whereas in the third dorsal of this taxon, the transverse process has a slight dorsal orientation, so that its dorsal surface is not exposed in lateral view. Another character that supports this interpretation is the location of the parapophysis in the middle of the centrum, as in the second dorsal of *Allosaurus* (Madsen 1976), whereas in the third dorsal the parapophysis is located on the base of the neural arch (Figure 7).

#### 5.5.1 Atlas

The atlas (MPEF-PV 1157) is an anteroposteriorly short element. In anterior view, the vertebral body has a square contour at its ventral half. The anterior surface of the centrum has a deep concavity that articulates with the occipital condyle. Within this concavity, the dorsal sector bears an oval perforation separated from the neural canal by a thin bridge of bone (Figure 8(A),(C)). In posterior view, the centrum is dorsally concave and ventrally convex. The dorsal concavity corresponds to the articulation with the odontoid process of the axis. The neural arch is as high as the centrum. Anteriorly and laterally to the neural canal there is a pair of rounded prominences. Ventrally to each postzygapophysis, the neural arch bears

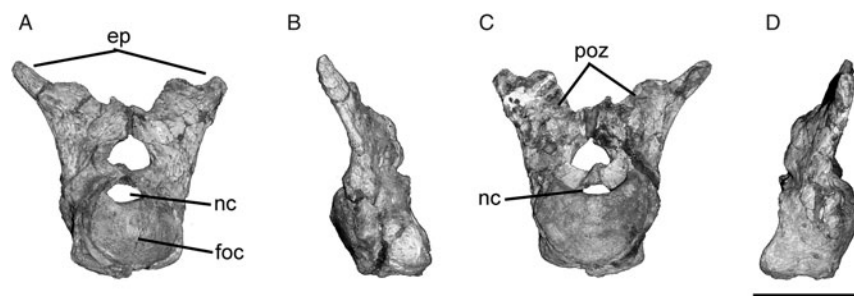


Figure 8. *Tyrannotitan chubutensis* atlas (MPEF-PV 1157) photographs in (A) anterior view, (B) right lateral view, (C) posterior view and (D) left lateral view. Note: Scale bar is 10 cm; see text for abbreviations.

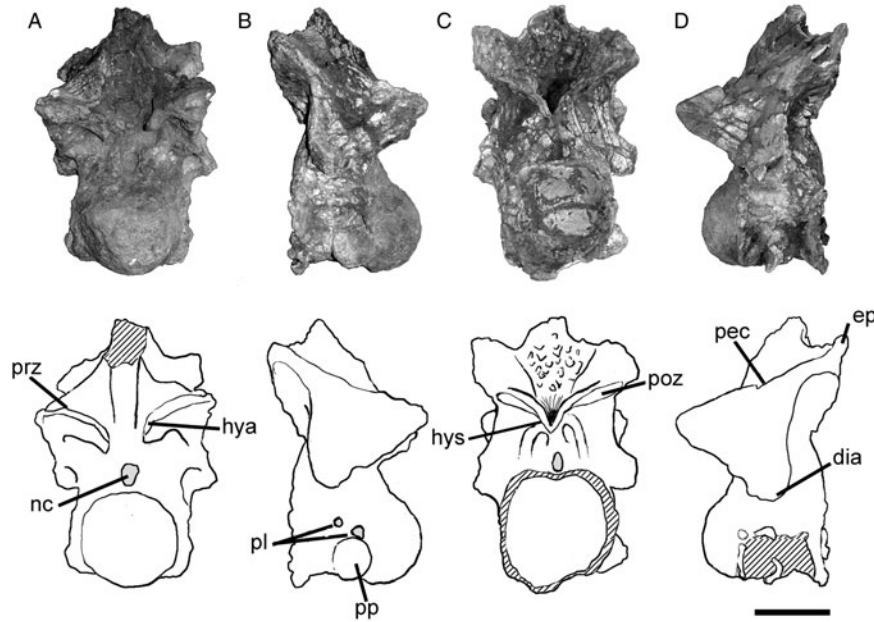


Figure 9. *Tyrannotitan chubutensis* seventh cervical vertebra (MPEF-PV 1157) photographs and line drawings in (A) anterior view, (B) right lateral view, (C) posterior view and (D) left lateral view. Note: Scale bar is 10 cm; see text for abbreviations.

a rounded and well-marked fossa. The postzygapophyses are oriented medioventrally (Figure 8(C)). The epiphyses are well developed (Figure 8), as in *Torvosaurus* (BYU-VP 725/4884), *Majungasaurus* (O'Connor 2007) and *Acrocanthosaurus* (NCSM 14345).

### 5.5.2 Seventh cervical

The centrum of this vertebra (MPEF-PV 1157) is strongly opisthocoelic, having a hemispherical anterior articular surface (Figure 9), as in *Giganotosaurus* (MUCPV-Ch 1), but unlike that of *Allosaurus* (UMNH-PV 8354) in which the opisthocoely is less developed. The ventral surface is concave in lateral view. The parapophysis is large and rounded, and located at the anteroventral corner of the lateral surface of the centrum, immediately behind the anterior articular face. This vertebra has two pleurocoels on its lateral surface (Figure 9(B)), as in *Carcharodontosaurus saharicus* (NCSM 18166) and *Giganotosaurus* (MUCPV-Ch 1). The anterior pleurocoel is located dorsally to the parapophysis, is larger than the posterior pleurocoel and is separated from the posterior pleurocoel by a thin oblique sheet of bone. The posterior surface of the centrum is nearly circular, except for its flattened dorsal margin below the neural canal. The prezygapophyses are wide and dorsomedially oriented. The medial edge of each prezygapophysis is ventrally curved forming a rudimentary hypantrum (Figure 9(A)), which is not as developed as in the dorsal vertebrae.

The diapophysis is triangular in lateral view (Figure 9(B),(D)), as in *Giganotosaurus* (MUCPV-Ch 1), *Mapusaurus* (MCF-PVPH 108.90) and *Carcharodontosaurus*

*saharicus* (NCSM 18166), and is lateroventrally directed. The prezygodiapophyseal lamina is supported by two accessory laminae: the anterior of which is more developed. In posterior view, dorsal to the neural canal, there is a small vertical lamina that supports the base of the 'U-shaped' hyposphene. On each side of this lamina, over the neural canal, the neural arch bears small circular fossae that are bounded laterally by a curved lamina, which comes from the vertebral centrum and connects to the lateral wall of the hyposphene (Figure 9(C)). Dorsal to postzygapophyses, a rhomboid deep depression occupies the entire posterior surface of the neural spine, at the centre of which is distinguished the ligament scar. The epiphyses are pointed and well developed on the dorsal surface of each postzygapophysis (Figure 9(D)). The robust neural spine has a quadrangular cross section at its base, as in *Giganotosaurus* (MUCPV-Ch 1) and *Mapusaurus* (MCF-PVPH 108.90). At the base of its anterior surface there are ligament scars.

### 5.5.3 First dorsal

The centrum of the first dorsal (MPEF-PV 1157) is larger but less opisthocoelic than in the seventh cervical. The kidney-shaped parapophyses are located anteroventrally on the lateral sides of centrum. Dorsally to each parapophysis, the centrum bears a large oval pleurocoel (Figure 10(B),(D)). The posterior surface of the centrum has a perfectly circular outline. The ventral surface is concave in lateral view. The neural arch is higher and anteroposteriorly shorter than that of the seventh cervical vertebra. The neural canal is oval, being higher than wide.

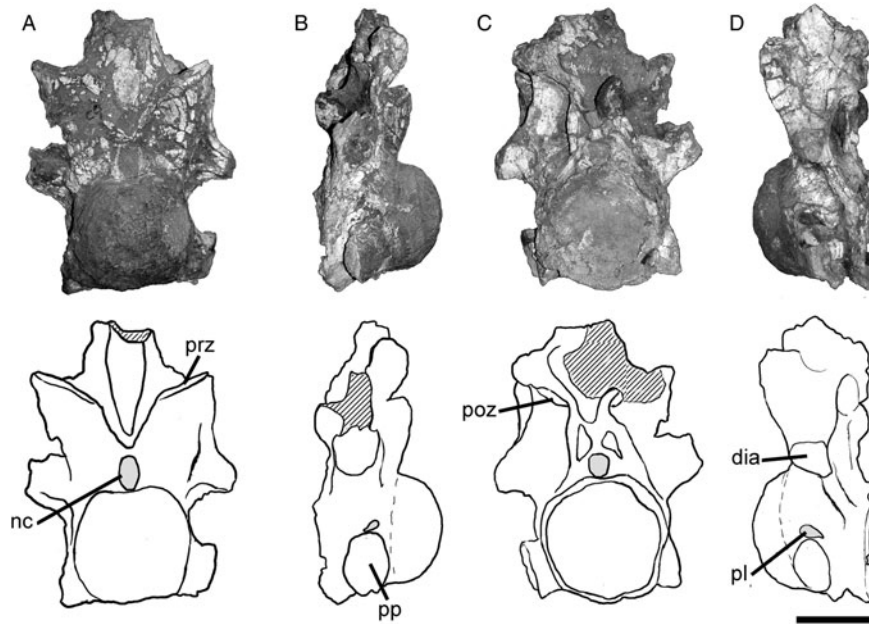


Figure 10. *Tyrannotitan chubutensis* first dorsal vertebra (MPEF-PV 1157) photographs and line drawings in (A) anterior view, (B) right lateral view, (C) posterior view and (D) left lateral view. Note: Scale bar is 10 cm; see text for abbreviations.

The prezygapophyses are dorsally positioned, on the neural arch, with a wide hypantrum developed ventral to them (Figure 10(A)). The neural spine is robust, with a square-shaped base in cross section. The transverse processes are more laterally than ventrally directed. The prezygapophyses, as the postzygapophyses, face dorsally as in the rest of the dorsal vertebrae. The hyposphene is well developed and has a short medial lamina at its ventral end that extends down to the dorsal edge of the neural canal. On both sides of the above-mentioned lamina, deep fossae are present. These are laterally bounded by a pair of curved laminae that have a similar disposition to that described of the seventh cervical, but are proportionally more robust (Figure 10(C)). These same laminae are present in *Mapusaurus* (MCF-PVPH 108.82) but in this taxon they are less developed than in *Tyrannotitan*.

#### 5.5.4 Second dorsal

In the second dorsal vertebra, only the neural arch has been preserved (MPEF-PV 1156), lacking neural spine. The transverse process is laterally directed, so that its dorsal surface is exposed in lateral view. The centroprezygapophyseal lamina is subvertically oriented and merges with the anterior centrodiapophyseal lamina. The resultant lamina extends along the neural arch towards the parapophysis (Figure 11), as in the second dorsal of *Acrocanthosaurus* (Harris 1998), *Allosaurus* (Madsen 1976) and in an anterior dorsal of *Mapusaurus* (MCF-PVPH 108.82). The parapophysis is located at mid height of the neural arch. The centroprezygapophyseal fossa

(*sensu* Wilson et al. 2011) is shallower than in more posterior dorsal vertebrae. The posterior centrodiapophyseal lamina is more robust than the anterior centrodiapophyseal lamina and is vertically oriented. Both laminae delimit a triangular and deep centrodiapophyseal fossa. At the ventral region of this fossa there is a low accessory lamina that runs anteroposteriorly (Figure 11).

#### 5.5.5 Third dorsal

In this vertebra (MPEF-PV 1156) only the neural arch and part of the centrum have been preserved. The neural arch is anteroposteriorly longer than that of the second dorsal, in part because the transverse process becomes more posterodorsally oriented and the prezygapophysis is more anteriorly projected, surpassing the anterior border of the vertebral centrum. This trend among the transverse processes and prezygapophysis is accentuated in subsequent vertebrae. Consequently, along this series the centroprezygapophyseal fossa becomes progressively wider and deeper in posterior dorsal vertebrae. The parapophysis is located at the base of the neural arch. As in the second dorsal, the anterior centrodiapophyseal lamina merges with the centroprezygapophyseal and the resultant lamina extends over the neural arch dorsal to the parapophysis. The accessory lamina is more prominent and better defined than in the second dorsal (Figure 11). This lamina is absent in the anterior dorsal vertebra of *Mapusaurus* (MCF-PVPH 108.82) and *Allosaurus* (UMNH-VP 8334). In *Acrocanthosaurus* (SMU-74646 4-17; Harris 1998), there are two thin accessory laminae in

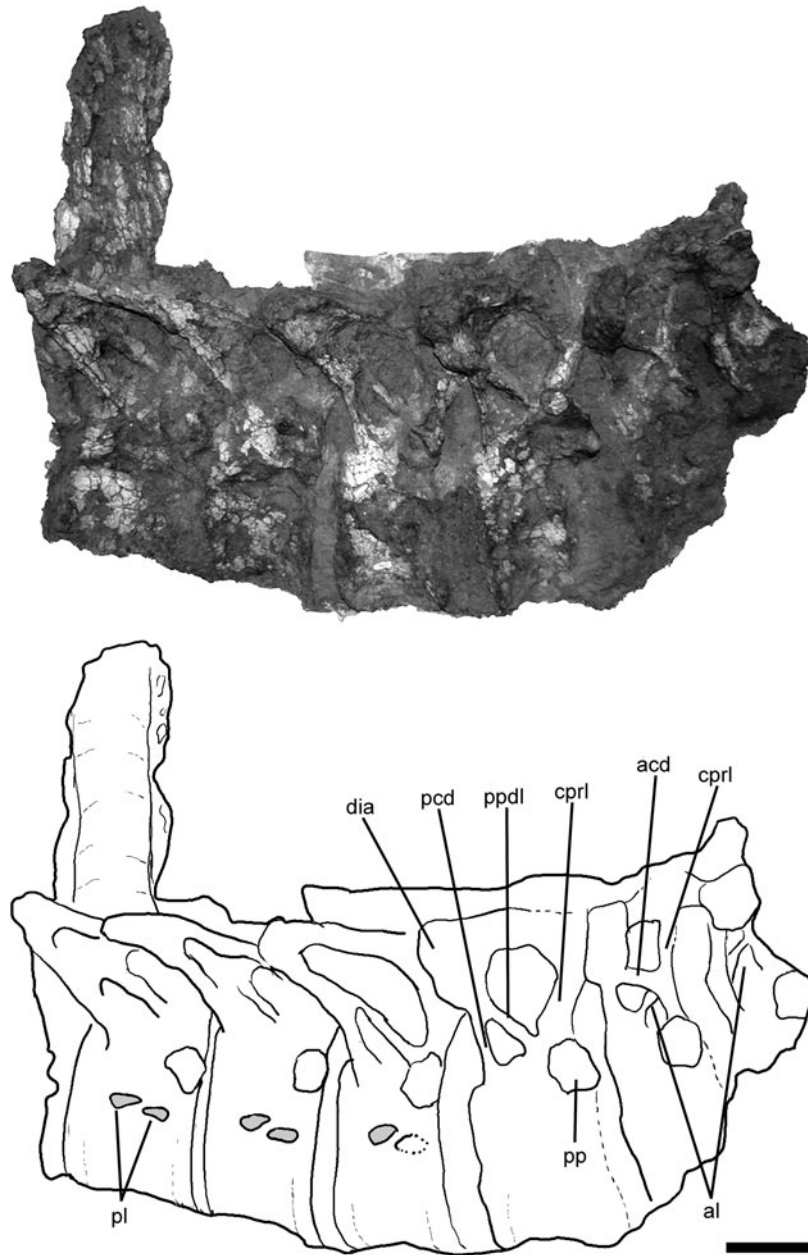


Figure 11. *Tyrannotitan chubutensis* articulated second dorsal to seventh dorsal vertebrae (MPEF-PV 1156) photographs and line drawings in right lateral view. Note: Scale bar is 10 cm; see text for abbreviations.

the third dorsal vertebra, which resemble that of *Tyrannotitan*, although they are much less developed. The parapophysis is dorsoventrally elongated.

#### 5.5.6 Fourth dorsal

The fourth dorsal vertebra is represented by fragments of the centrum and neural arch in both holotype and paratype (Figures 11 and 12). The centrum is tall, with flat and ovoid articular surfaces, dorsoventrally elongated and with a concave margin under the neural canal. The centrum is

spool shaped, ventrally concave in lateral view and without a ventral keel. The centrum bears two pleurocoels on its lateral surface, which are anteroposteriorly aligned and separated by a thin oblique lamina (Figure 12), as in *Giganotosaurus* (MUCPV-Ch 1) and *Acrocanthosaurus* (Harris 1998). The neural canal is dorsoventrally elongated. The prezygapophysis faces dorsomedially. The hypantrum is thin walled, and delimits the medial margin of the deep centroprezygapophyseal fossae. These fossae are laterally limited by the centroprezygapophyseal laminae (Figure 12(A)). The neural arch has the same

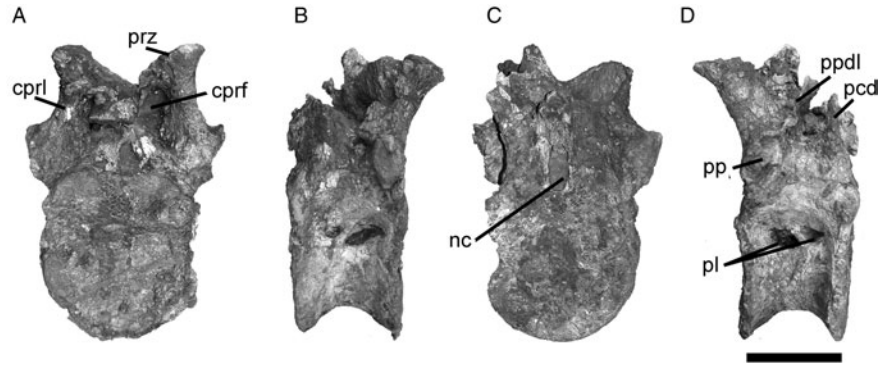


Figure 12. *Tyrannotitan chubutensis* fourth dorsal vertebra (MPEF-PV 1157) photographs in (A) anterior view, (B) right lateral view, (C) posterior view and (D) left lateral view. Note: Scale bar is 10 cm; see text for abbreviations.

height as the centrum. The centroprezygapophyseal lamina is shorter and more robust than in the preceding vertebrae. The anterior centrodiaepophyseal lamina reaches the dorsal border of the parapophysis and does not merge to the centroprezygapophyseal lamina. Therefore, in the fourth dorsal (and in more posterior vertebrae), this lamina is referred as parapodiaepophyseal lamina (Figure 11). In this vertebra, and in the subsequent dorsal vertebrae, there is no evidence of the accessory laminae described for the second and third dorsals. The centroprezygapophyseal fossa is wider than the centrodiaepophyseal fossa, whereas in the second dorsal both fossae are similarly developed. This trend is accentuated in the subsequent posterior vertebrae. The parapophysis is dorsoventrally elongated and is located at the anterior border of the neural arch.

#### 5.5.7 Fifth dorsal

The fifth dorsal vertebra lacks the neural spine (MPEF-PV 1156) (Figure 11). It has two aligned pleurocoels on each lateral side of the centrum. In lateral view, the tip of the transverse process surpasses the posterior border of the

centrum. The centroprezygapophyseal lamina is as robust as the same in the fourth dorsal, expanding to the base of the prezygapophysis. As in the precedent vertebrae, the centrodiaepophyseal lamina is vertically oriented. The parapophysis has a circular outline.

#### 5.5.8 Sixth dorsal

Two centra with part of the neural arch have been preserved of the sixth dorsal, belonging to holotype and paratype (Figures 11 and 13). The centrum is tall, amphiplatyan and ventrally concave in lateral view. Both pleurocoels are anteroposteriorly elongated and located on the dorsal region of the lateral surface of the centrum. The neural canal is dorsoventrally elongated. The prezygapophysis faces dorsally and below them there are two deep centroprezygapophyseal fossae, limited laterally by the robust centroprezygapophyseal laminae and medially by the hypantrum walls (Figure 13(A)). Over the anterior border of the prezygapophysis there are two rounded pneumatic pits, which are also present in *Giganotosaurus* (MUCPV-Ch 1), *Mapusaurus* (MCF-PVPH 108.84) and *Allosaurus*

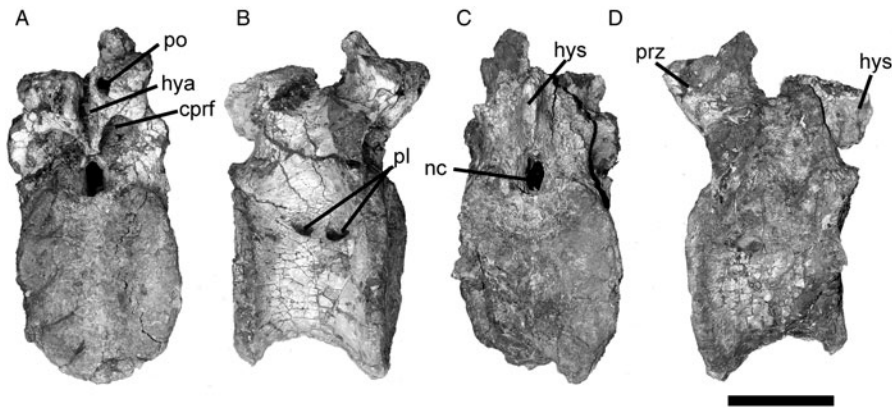


Figure 13. *Tyrannotitan chubutensis* sixth dorsal vertebra (MPEF-PV 1157) photographs in (A) anterior view, (B) right lateral view, (C) posterior view and (D) left lateral view. Note: Scale bar is 10 cm; see text for abbreviations.

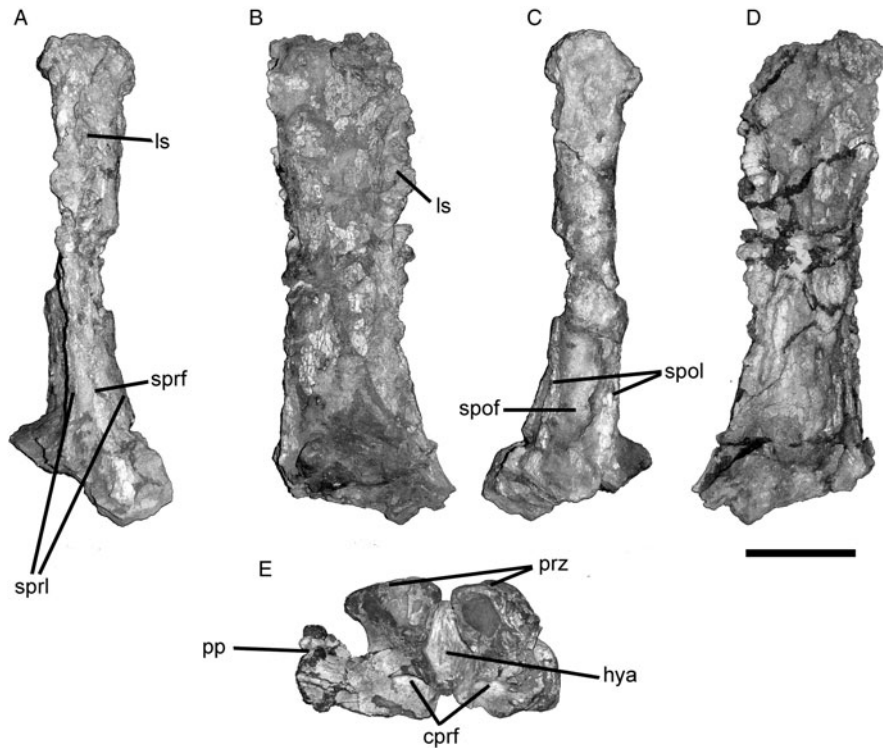


Figure 14. *Tyrannotitan chubutensis* eighth dorsal vertebra (MPEF-PV 1157) photographs in (A) anterior view, (B) right lateral view, (C) posterior view, (D) left lateral view of the isolated neural spine and (E) anterior view of a fragment of the neural arch. Note: Scale bar is 10 cm; see text for abbreviations.

*fragilis* (UMNH-VP 10108). The hyposphene–hypantrum facets are well developed and dorsoventrally elongated. The parapophysis is located at the anteroventral border of the neural arch (Figure 11). The centrodiapophyseal lamina is robust and the parapodiapophyseal is very reduced. The transverse process is strongly posterodorsally directed.

#### 5.5.9 Seventh dorsal

Remains of the seventh dorsal have been preserved on both the holotype and the paratype. The transverse process is more posterodorsally oriented and the centroprezygapophyseal lamina is shorter and more robust than in the sixth dorsal vertebra (Figure 11). The parapodiapophyseal lamina is weakly developed in comparison with the posterior centrodiapophyseal lamina. The neural spine is as high as the centrum plus the neural arch. The neural spine has strongly developed ligament scars on the dorsal region of its anterior surface, as in *Mapusaurus* (MCF-PVPH 108) and *Acrocantnosaurus* (Harris 1998). The centrum bears two pleurocoels on the dorsal region of its lateral surface.

#### 5.5.10 Eighth? dorsal

An isolated neural spine (MPEF-PV 1156) (Figure 14(A)–(D)) and part of a neural arch (MPEF-PV 1157) (Figure 14

(E)) were assigned with doubts to the eighth dorsal vertebra. The centroprezygapophyseal fossae are strongly reduced and restricted to the base of the parapophysis (Figure 14(E)). The hypantrum is rhomboid shaped, being wider at its central sector than in the sixth dorsal. The parapophysis is laterally directed, and has a pointed projection at its dorsal end. The neural spine is subrectangular in lateral view, with a central anteroposterior and lateromedial constriction. The ligament scars are strongly developed, having rounded anterolateral projections and being restricted to the dorsal half of the neural spine. The spinoprezygapophyseal laminae ventrally delimit a wide spinoprezygapophyseal fossa (Figure 14(A),(C)). The posterior ligament scars are not as developed as those of the anterior surface.

#### 5.5.11 Ninth? dorsal

An isolated neural spine (MPEF-PV 1156) was assigned with doubts to the ninth dorsal vertebra. The overall morphology is very similar to that assigned to the eighth dorsal vertebra, but is higher and more slender. The pneumatic openings are well developed under each prezygapophysis. The right spinoprezygapophyseal lamina has a bifurcation with a small anterolateral lamina. The transverse process is dorsally oriented, but only a fragment

of this process has been preserved. The anterior ligament scar is strongly developed and restricted to the dorsal half of the spine.

#### 5.5.12 Tenth dorsal

The 10th dorsal vertebra has been almost completely preserved (MPEF-PV 1156) (Figure 15). The centrum is spool shaped and bears two ovoid pleurocoels. These are anteroposteriorly aligned and, unlike in the anterior dorsals, located within a deep and anteroposteriorly elongated fossa. The transverse process is laterally directed, as in the last dorsal vertebra of *Allosaurus* (Madsen 1976). The posterior centrodiaepophyseal lamina is robust and reaches the anterior margin of the postzygapophysis. The lateral border of the postzygapophysis is ventrally curved, covering laterally the prezygapophysis of the subsequent vertebra (preserved in articulation), as in *Giganotosaurus* (MUCPV-Ch 1), *Acrocanthosaurus* (Harris 1998), *Majungasaurus* (O'Connor 2007) and *Carnotaurus* (MACN-CH 894). The morphology of the neural spine is very similar to that of the preceding dorsal vertebrae.

#### 5.5.13 Eleventh dorsal

The 11th dorsal vertebra (MPEF-PV 1156) is almost completely preserved and articulated with the 10th dorsal

(Figure 15). In posterior aspect, the articular surface has a subcircular outline as in the posterior dorsal vertebrae of *Giganotosaurus* (MUCPV-CH 1) and *Allosaurus* (Madsen 1976). As in the 10th dorsal, the pleurocoels are located within a deep and anteroposteriorly elongated fossa. The parapophyses are dorsoventrally elongated. The transverse processes are laterally directed. The centroprezygapophyseal lamina is short and robust. The parapodiapophyseal lamina is an oblique and very thin sheet of bone. The posterior centrodiaepophyseal lamina is vertically oriented and thinner than in the 10th dorsal. The postzygapophysis has its lateral margin ventrally curved, as in the 10th dorsal. The spinopostzygapophyseal laminae are markedly robust at their base, and both delimit a deep spinopostzygapophyseal fossa. Between both postzygapophyses, only a fragment of the hyposphene has been preserved in this vertebra.

#### 5.5.14 Twelfth dorsal

Only an isolated vertebral centrum is known from the 12th dorsal vertebra (MPEF-PV 1157). The posterior articular surface has a circular contour. The anterior pleurocoel is larger than the posterior pleurocoel. The left side of the centrum has preserved the base of an oblique anterior centrodiaepophyseal lamina and a vertical posterior centrodiaepophyseal lamina. Unlike the more anterior dorsal vertebrae, this vertebra has a wide ventral furrow.

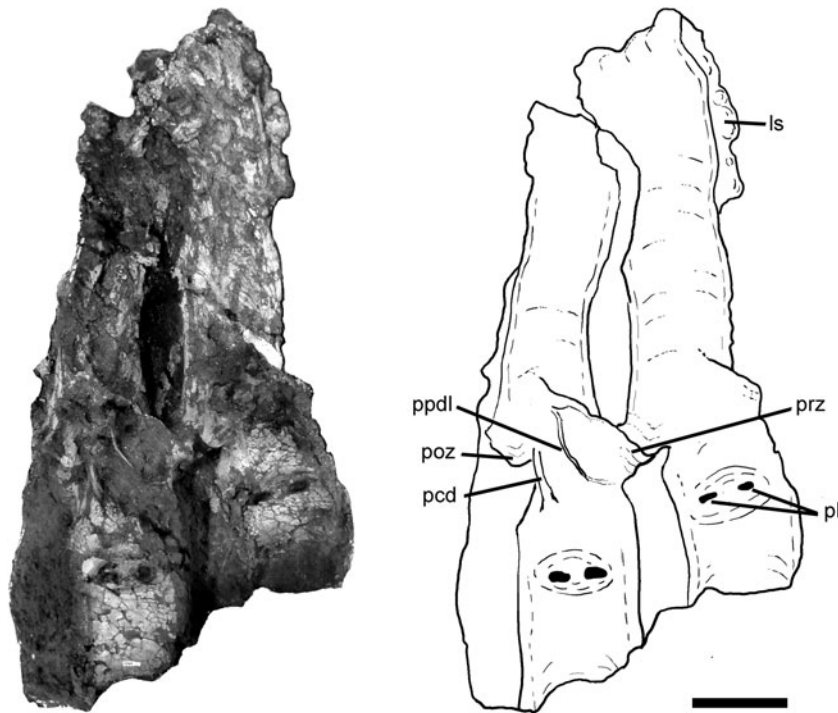


Figure 15. *Tyrannotitan chubutensis* articulated 10th and 11th dorsal vertebrae (MPEF-PV 1156) photographs and line drawings in right lateral view. Note: Scale bar is 10 cm; see text for abbreviations.

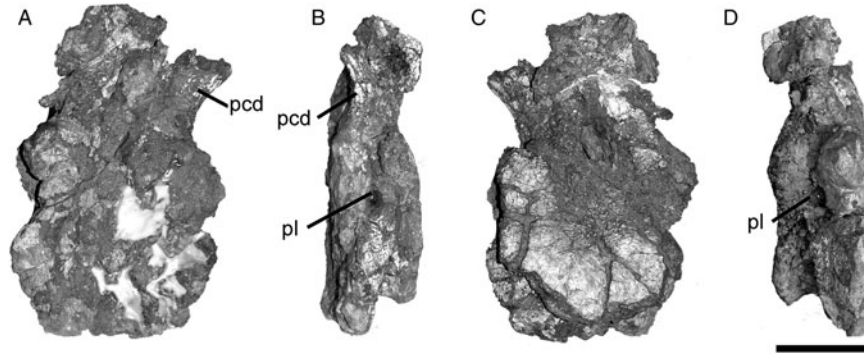


Figure 16. *Tyrannotitan chubutensis* 14th dorsal vertebra (MPEF-PV 1157) photographs in (A) anterior view, (B) right lateral view, (C) posterior view and (D) left lateral view. Note: Scale bar is 10 cm; see text for abbreviations.

#### 5.5.15 Thirteenth dorsal

Only the isolated centrum of the 13th dorsal vertebra has been preserved (MPEF-PV 1157). As in the 12th dorsal vertebra, the articular surfaces have a subcircular outline, the anterior pleurocoel is more developed than the posterior, and the centrum has a wide ventral furrow. The neural canal is rounded, instead of being dorsoventrally elongated as in the most anterior dorsal vertebrae.

#### 5.5.16 Fourteenth dorsal

The isolated vertebral centrum of the 14th vertebra has been preserved (MPEF-PV 1157) (Figure 16), as well as an isolated neural spine (MPEF-PV 1156) (Figure 17). The centrum is anteroposteriorly shorter than in the 12th and 13th vertebrae. Both anterior and posterior articular

surfaces are rounded, but the posterior one is smaller, which matches the size of the first sacral centrum. There is only one rounded pleurocoel on each lateral surface of the centrum (Figure 16(B),(D)). The posterior centrodiapophyseal lamina (only preserved on the left side) is anterodorsally directed, as in the 14th dorsal of *Allosaurus* (Madsen 1976) (Figure 16(B)). The hypantrum is well developed and dorsomedially elongated. The neural spine is anteroposteriorly shorter than that of the 10th and 12th dorsal vertebrae, as in *Allosaurus* (Madsen 1976) and *Tyrannosaurus* (Brochu 2003). The anterior ligament scar is strongly developed in this vertebra. The neural spine is anterodorsally oriented (Figure 17), as in the 14th dorsal vertebra of *Allosaurus* (Madsen 1976), *Sinraptor* (Currie and Zhao 1993) and *Aerosteon* (Serenio et al. 2008).

#### 5.5.17 Sacrum

A neural spine, found in articulation with the neural spine of the 14th dorsal (MPEF-PV 1156) (Figure 17), has been preserved from the sacrum of the holotype, as well as two fragments of fused sacral centra of the paratype (MPEF-PV 1157) (Figure 18).

The lateral surface of the neural spine is partially covered by a fragment of the left ilium. The spine is anteroposteriorly wider than in the 14th dorsal and has the posterior ligament scar strongly developed. As in *Giganotosaurus* (MUCPV-Ch 1), there is no evidence of fusion between the sacral neural spines.

The two preserved sacral fragments of the paratype include the left half of the first and a small part of the second sacral centrum, which are fused and have clear evidence of deformation, and a fused sequence of the third, fourth and fifth sacral centra. The sacrum is ventrally concave and medially compressed, as in *Giganotosaurus* (MUCPV-Ch 1), *Carnotaurus* (MACN-CH 894) and *Ceratosaurus* (Gilmore 1920) (Figure 18(A)–(C)). The lateral surface of the first sacral centrum bears a medial longitudinal ridge. The base of the neural arch has been

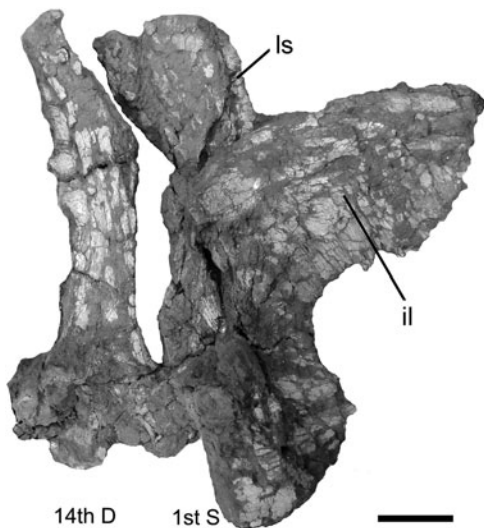


Figure 17. *Tyrannotitan chubutensis* articulated neural spines of 14th dorsal vertebra and 1st sacral vertebra (MPEF-PV 1156) photographs in left lateral view. Note: Scale bar is 10 cm; see text for abbreviations.

preserved and is located over the posterior half of the centrum. This vertebra lacks pleurocoels, but it has a pneumatic recess and small opening at the base of the neural arch (Figure 18(A)). The ventral surface, although incomplete seems to be transversely compressed. The third centrum is the smallest of the sacral series. The contact between the third and fourth centra is the lateromedially narrowest contact of the sacral series. The fourth sacral has the posterior surface expanded with respect to the anterior surface and has a pleurocoel on the posterodorsal region of the left lateral surface of the centrum (located within an anteroposteriorly elongated fossa) (Figure 18(A)). Sacral pleurocoels are known also in *Mapusaurus* (MCF-PVPH 108.209) and *Giganotosaurus* (MUCPV-Ch 1). The fifth sacral vertebra is the highest of the sacral series; its posterior articular surface is also expanded, and has a conspicuous pleurocoel on its lateral surface (as in the fourth sacral). The postzygapophysis preserved in this sacral centrum faces ventrally (Figure 18(D)).

#### 5.5.18 Anterior caudal

There is an almost complete anterior caudal vertebra (MPEF-PV 1156) (Figure 19), which has slight defor-

mation at the tip of its neural spine. This element is interpreted as belonging to the series between the 5th and 10th caudal vertebrae, giving the size difference between its centrum and that of the last sacral and the orientation of the zygapophyses.

The centrum is amphiplatyan. The margins of its articular surfaces are not complete, and they likely were more expanded than preserved, creating a spool-shaped centrum. There are anteroposteriorly elongated depressions ('pleurocoelic fossae') on the dorsal region of its lateral surface, as in *Giganotosaurus* (MUCPV-Ch 1) and *Mapusaurus* (MCF-PVPH 108.81). This differs from the condition of *Carcharodontosaurus saharicus* (Stromer 1931), which have actual pleurocoels in the anterior caudal vertebrae. The prezygapophyses face dorsomedially, at an angle of approximately 45th from the horizontal plane (Figure 19(A)). The spinoprezygapophyseal fossa is shallow between both spinoprezygapophyseal laminae. Over the dorsal half of the anterior surface of the neural spine, there is a ligament scar, which is less developed than in the posterior dorsal vertebrae. The transverse processes are robust and posterolaterally oriented. The anterior surface of the transverse process bears a longitudinal wide fossa, as in the anterior caudal vertebrae of *Giganotosaurus*

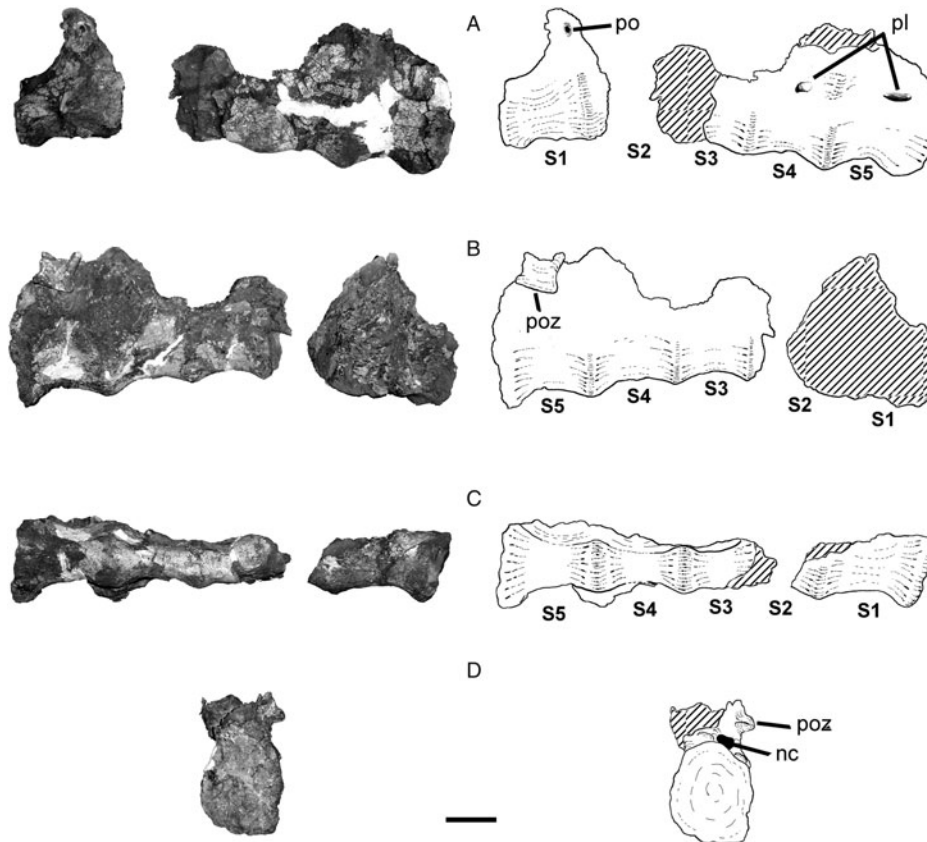


Figure 18. *Tyrannotitan chubutensis* sacrum (MPEF-PV 1157) photographs and line drawings in (A) left lateral view, (B) right lateral view, (C) ventral view and (D) posterior view. Note: Scale bar is 10 cm; see text for abbreviations.

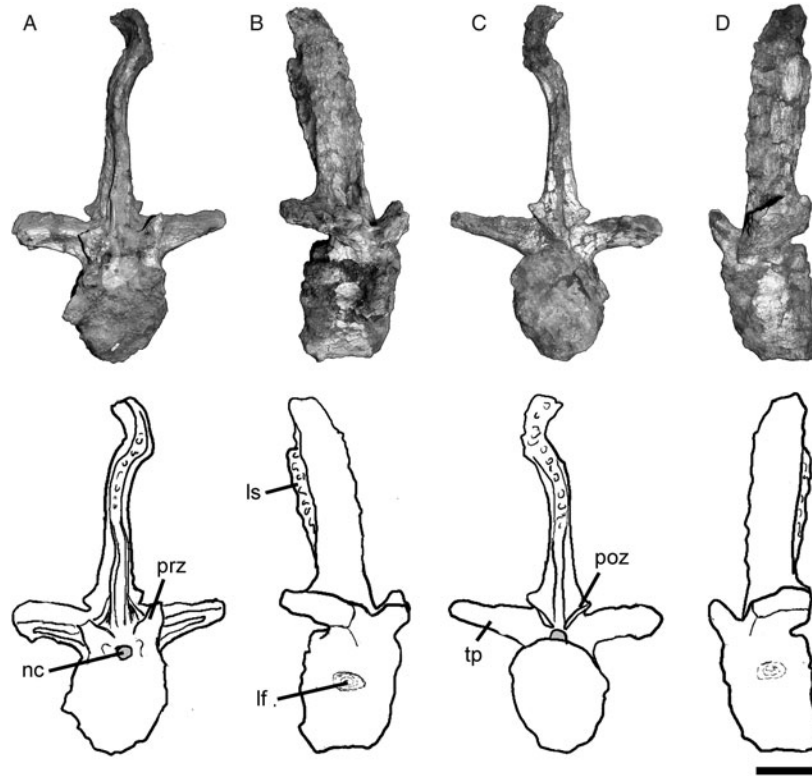


Figure 19. *Tyrannotitan chubutensis* anterior caudal vertebra (MPEF-PV 1156) photographs in (A) anterior view, (B) right lateral view, (C) posterior view and (D) left lateral view. Note: Scale bar is 10 cm; see text for abbreviations.

(MUCPV-Ch 1). The postzygapophyses faces ventrolaterally. Dorsal to the postzygapophyses and between both spinopostzygapophyseal laminae there is a deep spinopostzygapophyseal fossa, limited dorsally by a ligament scar, which is much more developed than the anterior scars (Figure 19(B),(D)). The neural spine is twice as tall as the centrum. There is no preserved hypantrum in this element, but there is a small hyposphene between the postzygapophyses, as in *Giganotosaurus* (MUCPV-Ch 1) and possibly in cf. *Veterupristisaurus* (MB R 1940: Rauhut 2011).

#### 5.5.19 Distal caudal

There is a fragmentary and isolated distal caudal vertebra preserved (MPEF-PV 1157) (Figure 20). Based on

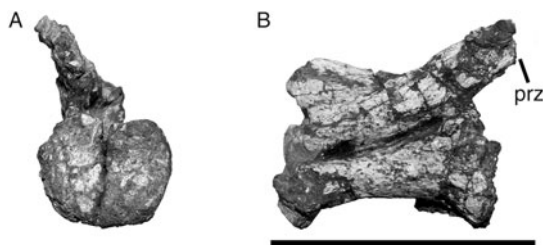


Figure 20. *Tyrannotitan chubutensis* distal caudal vertebra (MPEF-PV 1157) photographs in (A) anterior view and (B) right lateral view. Note: Scale bar is 10 cm; see text for abbreviations.

comparisons with the caudal series of *Allosaurus* (Madsen 1976), this element was interpreted as belonging to the series between the 30th and 35th caudal vertebrae. The centrum is laterally compressed, ventrally concave in lateral view and expanded at its articular surfaces. The anterior articular surface (the only one preserved) is wider than high. The lateral surface of the centrum bears an anteroposteriorly long depression. The preserved right prezygapophysis is laterodorsally projected and seems to have the spinoprezygapophyseal lamina extending as anteriorly as in *Veterupristisaurus* (to the midwidth of the base of the prezygapophysis; Rauhut 2011). In addition, the lamina that extends over the lateral surface of the prezygapophysis, which characterises *Veterupristisaurus* (Rauhut 2011), is absent in *Tyrannotitan*. The neural spine is low and anteroposteriorly extended.

#### 5.5.20 Ribs

Several ribs, mostly fragments, were recovered. They have no major differences with those of *Giganotosaurus* (MUCPV-Ch 1) and *Allosaurus* (Madsen 1976). A proximal fragment of an anterior dorsal rib (MPEF-PV 1157) lacks evidence of pneumatisation, as in *Mapusaurus* (Coria and Currie 2006) and *Sinraptor* (Currie and Zhao 1993). A complete posterior dorsal rib

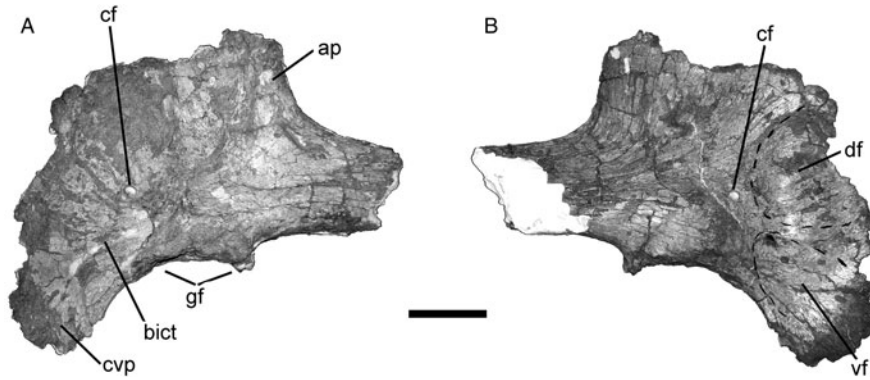


Figure 21. *Tyrannotitan chubutensis* left scapulocoracoid (MPEF-PV 1156) photographs in (A) lateral view and (B) medial view. Note: Scale bar is 10 cm; see text for abbreviations.

was recovered (MPEF-PV 1157), probably the 14th dorsal rib, based on the comparisons with *Allosaurus* (Madsen 1976). It is a short and recurved element with a flattened shaft. The capitulum is also flattened and its dorsomedial margin is formed by a lamina that connects to the subcylindrical tuberculum.

#### 5.5.21 Haemal arches

Seven haemal arches have been recovered from both the holotype and paratype specimens, five anterior and two distal. They are proximodistally long and laterally compressed elements. The haemal arch interpreted as the most anterior element is straight in lateral view, whereas the rest are posteriorly concave. The haemal canal is triangular in anterior view, and occupies approximately less than one-fifth of the total height of the bone, differing from the condition of the first 10 haemal arches of *Tyrannosaurus* in which the canal occupies at least one-fourth of their height (Brochu 2003). The haemal canal is dorsally closed by two oblique articular facets for the caudal vertebrae. Over the anterior and posterior margins of both proximal rami, there are rounded processes. The posterior process occupies a more distal position over the ramus than the anterior process.

#### 5.6 Scapulocoracoid

A left coracoid with the proximal third of the scapula fused was preserved (MPEF-PV 1156). Although this element is damaged, it has preserved the subcircular outline of the coracoid (Figure 21). The coracoid is a robust bone near the glenoid cavity, and becomes thinner towards the anterior and dorsal margins. The posteroventral process is well developed, as in *Giganotosaurus* (MUCPV-Ch 1), *Allosaurus* (UMNH-VP 9822), *Piatnitzkysaurus* (Bonaparte 1986) and *Carnotaurus* (MACN-CH 894). The anteroventral sector of the lateral surface of the coracoid

bears a long biceps tubercle (Figure 21(A)), as in *Tyrannosaurus* (Brochu 2003). This tubercle is represented by a straight low crest of about 9 cm long, being more pronounced at its posterodorsal end. The coracoid foramen is large and rounded, positioned in a central position on the lateral surface of the coracoid, as in *Giganotosaurus* (MUCPV-Ch 1), but unlike *Mapusaurus* (MCF-PVPH 108.71) in which the foramen is located near the glenoid cavity. This foramen perforates the bone obliquely, so that the medial opening is more posteriorly positioned than the lateral one. A broad fossa occupies most of the anterior region of the medial surface of the coracoid. This fossa is subdivided in two smaller fossae: one located dorsally and another located ventrally, being separated from each other by a low anteroposterior crest (Figure 21(B)).

Only the proximal scapula part was preserved, which, unlike *Mapusaurus* (MCF-PVPH 108.50; MCF-PVPH 108.71), is completely fused to the coracoid. The acromial process projects abruptly forming a straight angle with the dorsal margin of the scapular blade, as in *Mapusaurus* (Coria and Currie 2006), *Acrocanthosaurus* (Harris 1998) and most non-avian theropods. The anterolateral region of the acromion process is occupied by the subacromial fossa. The preserved portion of the scapular blade has a wide and rounded ventral border and a sharp dorsal margin.

#### 5.7 Humerus

Only the distal half of a right humerus has been preserved (MPEF-PV 1156). The distal end is preserved of the deltopectoral crest at the proximal end of the preserved anterior surface, which is anteromedially oriented as in *Mapusaurus* (MCF-PVPH 108.45). In contrast, *Allosaurus* (UMNH-VP 8157) and *Acrocanthosaurus* (NCSM 14345) have an anteriorly projected distal end of the deltopectoral crest. The humerus is lateromedially expanded at its distal end (Figure 22(A),(C)). At the medioventral region of the anterior surface, the humerus bears the proximal end of the

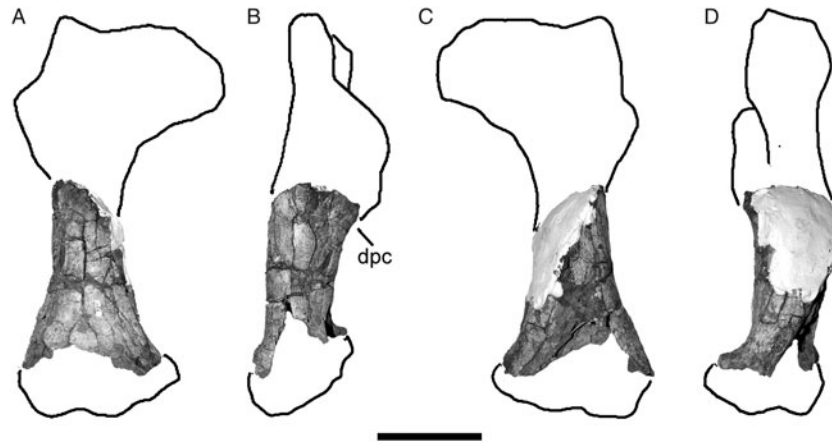


Figure 22. *Tyrannotitan chubutensis* right humerus (MPEF-PV 1156) photographs in (A) anterior view, (B) lateral view, (C) posterior view and (D) medial view. Note: Scale bar is 10 cm; see text for abbreviations.

fossa located between the radial and ulnar condyles (Figure 22(A)). This fossa has a triangular outline, as in *Mapusaurus* (MCF-PVPH 108.45) and *Torvosaurus* (BYU-VP 2002). In lateral view, it can be seen that the distal articular condyles are anteriorly projected (Figure 22 (B),(D)).

### 5.8 Radius

The right ulna cited by Novas et al. (2005) is reinterpreted here as a right radius, based on comparisons with *Acrocanthosaurus* (NCSM 14345) and *Allosaurus* (Madsen 1976; UMNH-VP unnumbered). In addition, a fragment of left radius has been preserved in the holotype.

The radius is a short and robust bone that is strongly curved, being posteriorly concave (Figure 23), as in *Acrocanthosaurs* (NCSM 14345) and *Mapusaurus* (MCF-PVPH-108.46), but unlike that of *Allosaurus* (Madsen 1976; UMNH-VP unnumbered). In anterior view the radius is straight. The shaft is subcircular in cross section

and the proximal end is expanded. The proximal articular surface, although partially eroded, has preserved an ovoidal contour, as in *Acrocanthosaurus* (NCSM 14345) and *Mapusaurus* (MCF-PVPH 108.46). The proximal expansion is laterally projected. The region of the radius on the medial surface where the ulna articulates is smooth and slightly depressed. The distal of the radius end is only moderately expanded.

### 5.9 Ilium

Two fragments of the left ilium were preserved (MPEF-PV 1156). One of them, preserved attached to the posteriormost dorsal and first sacral neural spines (Figure 17), corresponds to part of the preacetabular blade. The other fragment is interpreted here as the lateral wall of the postacetabular blade, which is lateromedially narrow. The posterior sector of this fragment is ventrally directed.

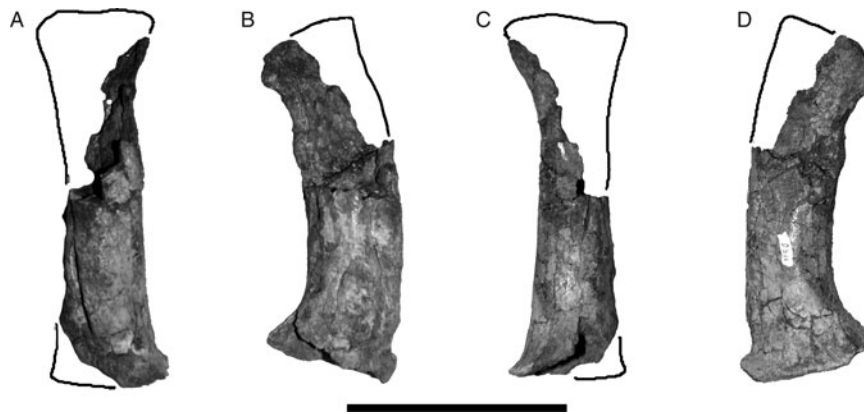


Figure 23. *Tyrannotitan chubutensis* right radius (MPEF-PV 1156) photographs in (A) anterior view, (B) lateral view, (C) posterior view and (D) medial view. Note: Scale bar is 10 cm; see text for abbreviations.

### 5.10 Pubis

Both pubic shafts have been preserved, lacking their proximal end and distal foot (MPEF-PV 1156) (Figure 24). The pubic shafts are straight in lateral view (Figure 24(B)), as in *Giganotosaurus* (MUCPV-Ch 1), but unlike *Carcharodontosaurus saharicus* (Stromer 1931) and *Acrocanthosaurus* (Harris 1998) in which these elements are anteriorly curved. In anterior or posterior view the pubic shaft has a sigmoid shape (Figure 24(A),(C)). The pubic symphysis is laminar and occupies the central third of the preserved region of the pubis. Distally to the symphysis and proximally delimited by pubic foot, a proximodistally enlarged pubic foramen is present. Proximal to the pubic symphysis the medial margins of the shaft are sharp, giving a tear-shaped cross section to this region of the pubic shaft. The distance between both iliac processes of both pubes and both ischia is approximately 40 cm, indicating the width of the hip in the holotype of *Tyrannotitan*.

### 5.11 Ischium

Both ischia have been almost completely preserved and articulated along their shafts (MPEF-PV 1156) (Figure 25). The ischia are not fused to each other, but in some parts the limit between the left and right element is not clear because of their poor preservation. The iliac peduncles, although incomplete, have a rectangular outline at their base. Based on the available material, it cannot be confirmed whether they had the pocket for the ischiatic peduncle of the ilium, as in *Giganotosaurus* (MUCPV-Ch 1) or *Mapusaurus* (Coria and Currie 2006). The pubic process is subrectangular, lateromedially compressed and

has the distinct ‘neck’ between the ischial body and the articular surface for the pubis, a feature also present in *Sinraptor* (Currie and Zhao 1993), *Allosaurus* (UMNH-VP 40-273) and *Carcharodontosaurus saharicus* (Rauhut 1995). The obturator processes are incompletely preserved on both ischia, but it can be observed that they were prominent and distally expanded, as in *Allosaurus fragilis* (UMNH-VP 40-273). The ischia also have preserved the obturator notch that separates the distal end of the obturator process and the ischiatic shaft (Figure 25(A),(C)), cited by Rauhut (1995) for *Sinraptor*, *Allosaurus*, *Carcharodontosaurus saharicus* and basal theropods.

Distally to the obturator processes, the ischiatic shafts are parallel to each other, as in *Allosaurus fragilis* (UMNH-VP 40-273), but unlike *Giganotosaurus* (MUCPV-Ch 1) in which the contact between both ischia is restricted to their distal ends. The ischiatic shaft is subcircular in cross section, and slightly expanded at its distal end. *Tyrannotitan*, however, lacks the distinct ischiatic foot present in *Neovenator* (Brusatte et al. 2008), *Concavenator* (Ortega et al. 2010) and *Acrocanthosaurus* (Harris 1998).

### 5.12 Femur

The femur is known by both femora of the holotype, and the right femur of the paratype. The femur is robust, straight in anterior view and anteriorly convex in lateral view (Figure 26). The femoral head is strongly upturned dorsomedially, as in *Giganotosaurus* (MUCPV-Ch 1), *Carcharodontosaurus saharicus* (Stromer 1931) and *Mapusaurus* (MCF-PVPH 108.203). The lesser trochanter

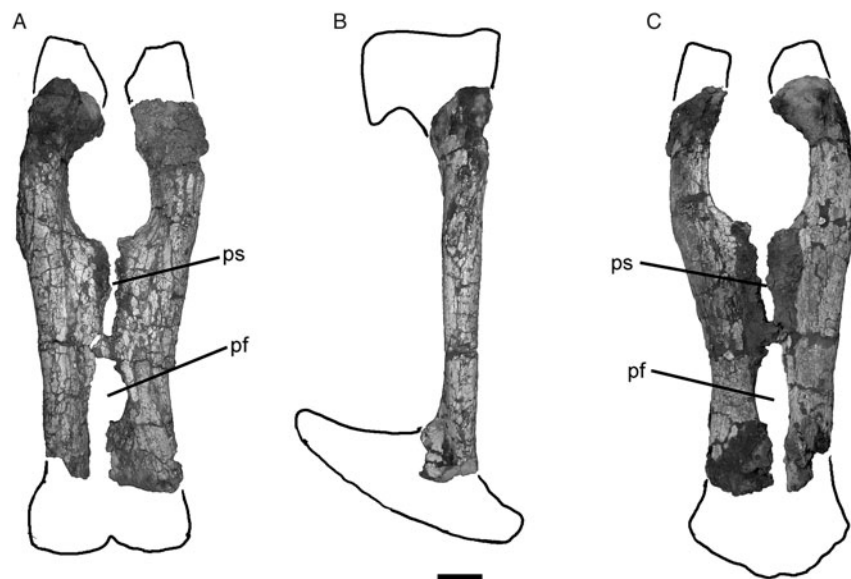


Figure 24. *Tyrannotitan chubutensis* articulated pubes (MPEF-PV 1156) photographs in (A) anterior view, (B) right lateral view and (C) posterior view. Note: Scale bar is 10 cm; see text for abbreviations.

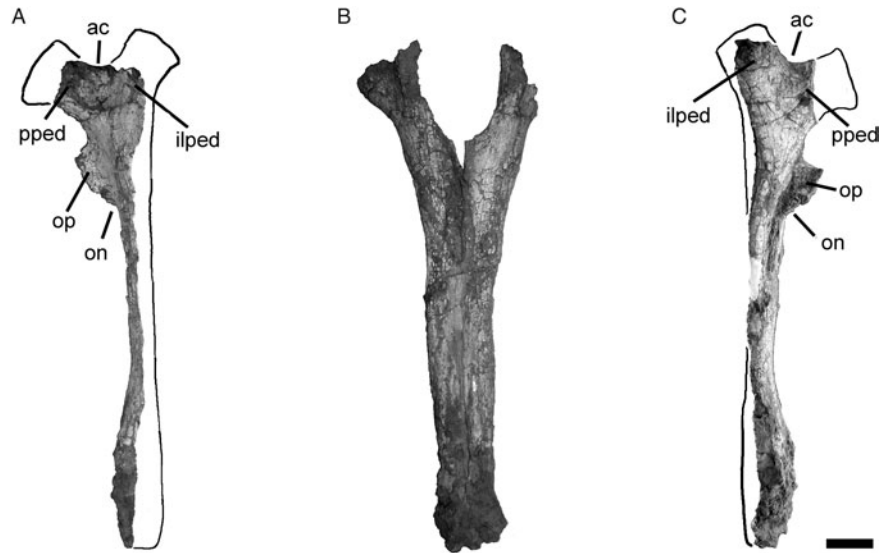


Figure 25. *Tyrannotitan chubutensis* articulated ischia (MPEF-PV 1156) photographs in (A) left lateral view, (B) anterior view and (C) right lateral view. Note: Scale bar is 10 cm; see text for abbreviations.

is proximally projected, but does not surpass the level of the greater trochanter (Figure 26(A)), as in *Concavenator* (Ortega et al. 2010) and *Carcharodontosaurus saharicus* (Stromer 1931). In contrast, the lesser trochanter of *Giganotosaurus* (MUCPV-Ch 1) is strongly reduced. Both lesser and greater trochanters are separated by a deep vertical notch. The lesser trochanter has a similar morphology to that of *Allosaurus fragilis* (UMNH-VP 12231), being subtriangular in lateral view and lateromedially robust. Distal to the lesser trochanter there is a rugose surface, probably for insertion of the iliofemoralis muscle. Distal to that surface there is a low pyramid-

shaped elevation: the ‘trochanteric shelf’ sensu Brochu (2003). The femoral shaft is lateromedially wider than anteroposteriorly long. The fourth trochanter is placed on the upper half of the posterior surface of the femoral shaft (Figure 26(B)), being a well-developed proximodistally elongated crest that is posteromedially projected. The fourth trochanter is more posteriorly projected and proximodistally longer than in *Mapusaurus* (MCF-PVPH 108.203) and *Giganotosaurus* (MUCPV-Ch 1), in which the fourth trochanter is reduced to a low crest. In *Tyrannotitan*, the fourth trochanter delimits posteriorly a distinct ovoid and proximodistally elongated fossa; the

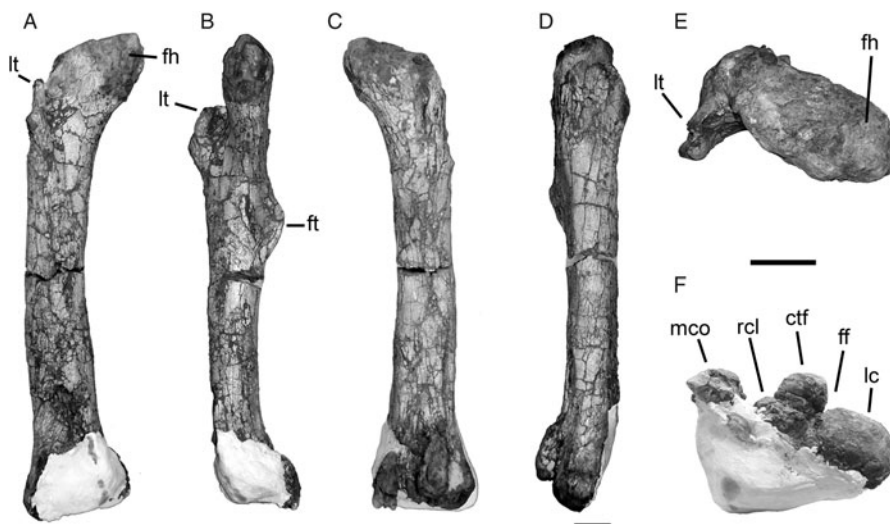


Figure 26. *Tyrannotitan chubutensis* right femur (MPEF-PV 1157) photographs and line drawings in (A) anterior view, (B) medial view, (C) posterior view, (D) lateral view, (E) proximal view and (F) distal view. Note: Scale bar is 10 cm; see text for abbreviations.

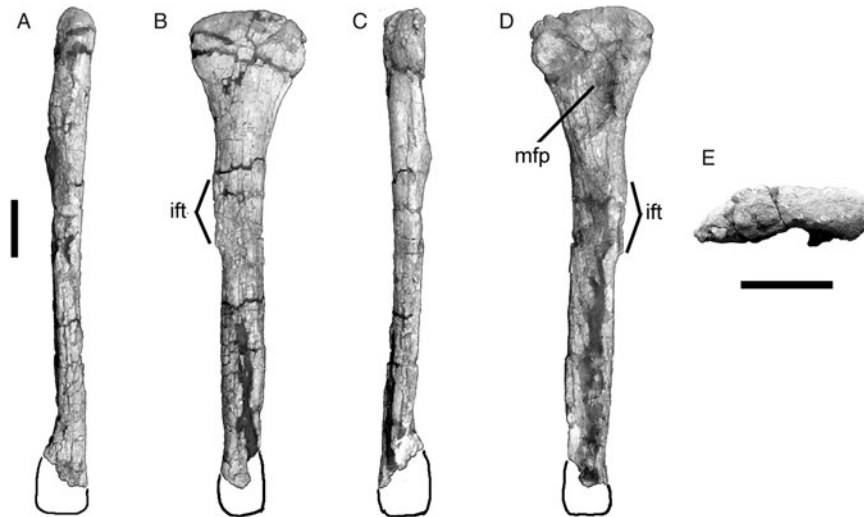


Figure 27. *Tyrannotitan chubutensis* left fibula (MPEF-PV 1157) photographs in (A) anterior view, (B) lateral view, (C) posterior view, (D) medial view and (E) proximal view. Note: Scale bar is 10 cm; see text for abbreviations.

insertion point of the *M. caudifemoralis longus* (Coria and Currie 2006).

Almost one-fourth of the anterior surface of the distal end of the femur is occupied by a well-developed mediolateral crest, as in *Mapusaurus* (Coria and Currie 2006) and *Giganotosaurus* (MUCPV-Ch 1), bounded by a low and wide depression with a medial projection. The fibular fossa, delimited by the lateral tibial condyle and the tibiofibular crest, extends proximally over the femoral shaft up to the proximal limit of the tibiofibular crest. This wide and shallow fossa has not been reported in other allosauroid theropods. In distal view, the posterior projections of the medial condyle and the tibiofibular crest are rounded (Figure 26(F)), differing from the pointed posterior projections of *Mapusaurus* (MCF-PVPH 108.55). The extensor fossa is shallow and broad, as in *Mapusaurus* (MCF-PVPH 108.55), and different from the narrow and deep fossa of *Allosaurus* (UMNH-VP 12231) and *Acrocanthosaurus* (Harris 1998; Currie and Carpenter 2000). The flexor fossa has a low ridge for the attachment of the cruciate ligaments, as in *Allosaurus* (UMNH-VP 12231) and *Acrocanthosaurus* (Harris 1998; Currie and Carpenter 2000). The lateral condyle is strongly developed and has a circular outline, as in *Mapusaurus* (MCF-PVPH 108.55). The lateral condyle and the tibiofibular crest are separated by a deep and very narrow fibular fossa as in *Mapusaurus* (MCF-PVPH 108.55), a condition absent in other allosauroid theropods.

### 5.13 Fibula

The preserved left fibula lacks its distal end (MPEF-PV 1156) (Figure 27). The proximal end is anteroposteriorly expanded, although the posterior projection is less

developed than in *Giganotosaurus* (MUCPV-Ch 1) and *Mapusaurus* (Coria and Currie 2006: fig. 30; right fibula figured as left). The proximal articular surface is smooth, as in *Giganotosaurus* (MUCPV-Ch 1). The proximomedial fossa is subovoid and tear-shaped, resembling the condition of *Giganotosaurus* (MUCPV-Ch 1), *Mapusaurus* (Coria and Currie 2006) and *Allosaurus fragilis* (UMNH-VP 6400). The anterior margin of the proximomedial fossa is posteriorly projected, covering a small part of the fossa (Figure 27(E)), a character absent in other allosauroids. The fibular shaft has a D-shaped cross section, with a flat medial surface. The *iliofibularis tubercle* is located on the distal region of the dorsal half of the anterior surface of the fibula (Figure 27(B),(D)). This tubercle is a proximodistally elongated ridge, resembling that condition of *Giganotosaurus* (MUCPV-Ch 1). Distal to the iliofibularis tubercle the anteroposterior width of the fibular shaft is constant.

### 5.14 Metatarsal II

Only the distal half of the left metatarsal II was preserved (MPEF-PV 1157) (Figure 28). This element is robust and has an expanded distal end, similar to that of *Allosaurus* (UMNH-VP 10142). The shaft has a subcircular cross section, with a slightly flattened medial surface for the contact with metatarsal III. On the ventral surface, the trochlea is separated from the shaft by a distinct lateromedial furrow (Figure 28(B)). Proximal to this furrow there are two tuberosities, a rounded distal tuberosity and an elongated proximal tuberosity. The collateral pits are deep and well delimited (Figure 28(D), (E)). The medial pit is deeper than the lateral pit, and is located at the distal sector of a marked fossa that occupies

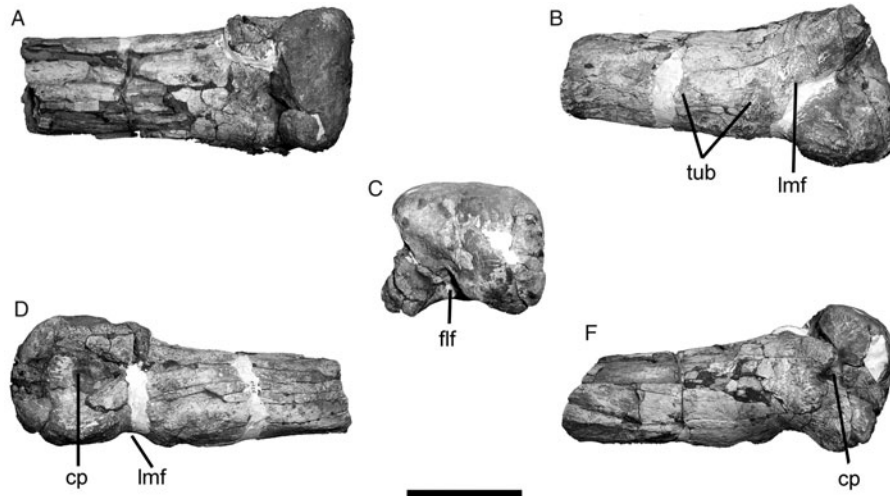


Figure 28. *Tyrannotitan chubutensis* left II metatarsal (MPEF-PV 1157) photographs in (A) dorsal view, (B) ventral view, (C) distal view, (D) lateral view and (E) medial view. Note: Scale bar is 10 cm; see text for abbreviations.

the entire lateral surface of the trochlea. The flexor fossa is deep and laterally displaced (Figure 28(C)), as in *Allosaurus fragilis* (UMNH-VP 10142) and *Sinraptor* (Currie and Zhao 1993), but unlike in *Torvosaurus* (BYU-VP 5147) in which this fossa is much shallower.

### 5.15 Pedal phalanges

We have reinterpreted the identity of the four preserved pedal phalanges of *Tyrannotitan* (see Novas et al. 2005) as the phalanges II-2, II-3, IV-2 and IV-3, all of which belong to the left pes of the paratype specimen (Figure 33).

#### 5.15.1 Phalanx II-2

This phalanx is robust and proximally expanded (Figure 29). The proximal articular surface is higher than wide and has a pronounced medial vertical sulcus. The ventral surface is flat and is separated from the trochlea by a transversal and laterally extensive furrow. On the proximal region of the lateral surface, there are two subcircular depressions, one dorsal and another ventral. The collateral ligamental pits are deep and located centrally on the lateral surfaces of the trochlea. In dorsal view, the lateral hemicondyle is more developed and distally projected than the medial hemicondyle.

#### 5.15.2 Phalanx II-3

This phalanx is a robust and recurved ungual that lacks the distal tip and part of the proximodorsal tubercle (Figure 30). It is asymmetrical in anterior view: the medial surface is located slightly dorsally with respect to the lateral surface. The ventral surface is mostly flat,

except for the presence of a transverse elongated furrow located on its proximal region. The collateral grooves are well marked, with the lateral groove more ventrally positioned than the medial one. These grooves run parallel to the ventral margin of the phalanx until the proximal third of this element, in which they are abruptly deflected ventrally. There is no evidence of proximal bifurcation of the collateral

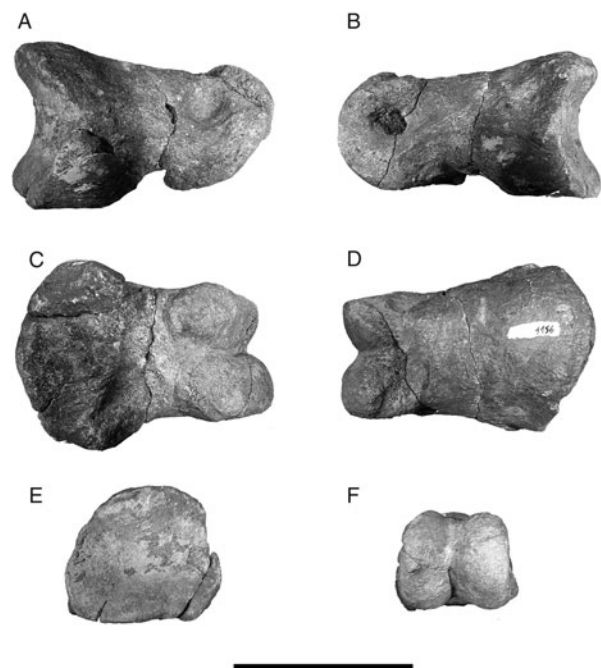


Figure 29. *Tyrannotitan chubutensis* phalanx II-2 (MPEF-PV 1157) photographs in (A) medial view, (B) lateral view, (C) ventral view, (D) dorsal view, (E) proximal view and (F) distal view. Note: Scale bar is 10 cm; see text for abbreviations.

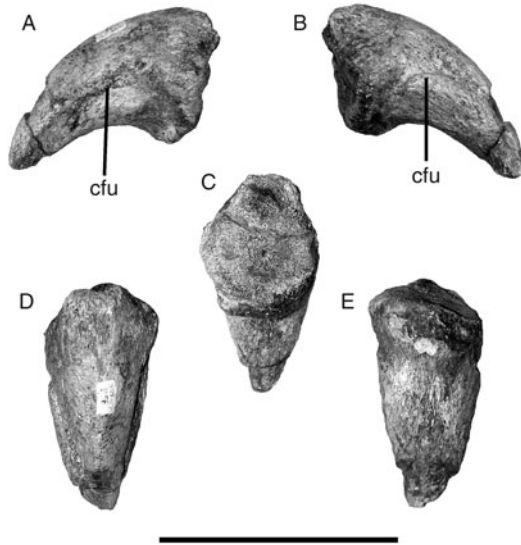


Figure 30. *Tyrannotitan chubutensis* phalange II-3 (MPEF-PV 1157) photographs in (A) lateral view, (B) medial view, (C) proximal view, (D) dorsal view and (E) ventral view. Note: Scale bar is 10 cm; see text for abbreviations.

grooves, contrasting with the condition of abelisaurids (Novas and Bandyopadhyay 2001). The proximal articular surface is subcircular and bears a rounded proximodorsal tubercle.

#### 5.15.3 Phalanx IV-2

This phalanx is short and robust and lacks part of the trochlea (Figure 31). The proximal articular surface is almost twice as wide as high. The ventral surface has a marked transversal furrow just proximal to the trochlea. Although this element is incompletely preserved, it can be determined that the medial hemicondyle was more developed than the lateral hemicondyle, as in *Allosaurus* (Madsen 1976) and *Sinraptor* (Currie and Zhao 1993).

#### 5.15.4 Phalanx IV-3

This phalanx is extremely short and lacks almost all the trochlea (Figure 32). The proximal articular surface has a straight ventral margin and continuous and curved lateral, medial and dorsal margins. As in the other non-terminal phalanges, it has ventral and dorsal transversal furrows that separate the trochlea from the rest of the phalanx.

## 6. Discussion

The combined elements of both holotype and paratype specimens of *Tyrannotitan chubutensis* (MPEF-PV 1156; MPEF-PV 1157) offer new information about the anatomy of this taxon and its diagnostic features, which improves

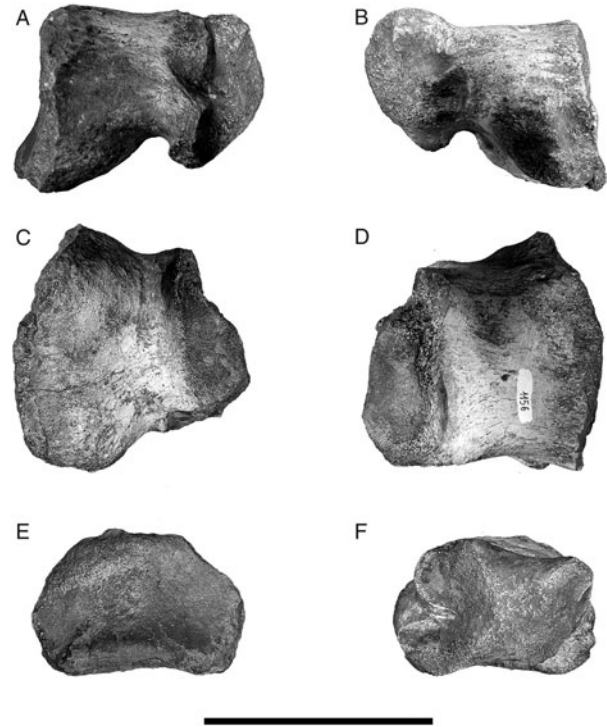


Figure 31. *Tyrannotitan chubutensis* phalange IV-2 (MPEF-PV 1157) photographs in (A) medial view, (B) lateral view, (C) ventral view, (D) dorsal view, (E) proximal view and (F) distal view. Note: Scale bar is 10 cm; see text for abbreviations.

our knowledge about poorly known anatomical regions in derived carcharodontosaurids. In this section we first discuss the diagnostic characters of *Tyrannotitan*, then we discuss the new data on the axial skeleton and the scapular girdle of carcharodontosaurids, and finally we present a phylogenetic analysis of Carcharodontosauridae (Figure 33).

### 6.1 Diagnostic features of *Tyrannotitan*

Novas et al. (2005) diagnosed *Tyrannotitan* based on three characters, only one of which is left in the emended diagnosis. These three characters are first discussed here, followed by a discussion of the four new autapomorphies found in this study.

#### 6.1.1 Characters in the original diagnosis

**6.1.1.1 Teeth with bilobated denticles in the mesial carinae.** This condition occurs in the teeth preserved in the holotype material of *Tyrannotitan* (MPEF-PV 1156) (Figure 34(A)) and some of the isolated teeth recovered at the site. Bilobated denticles are not present in all *Tyrannotitan* teeth and, therefore, this condition should be regarded as polymorphic among the available material. The reasons for this polymorphism could be intraspecific

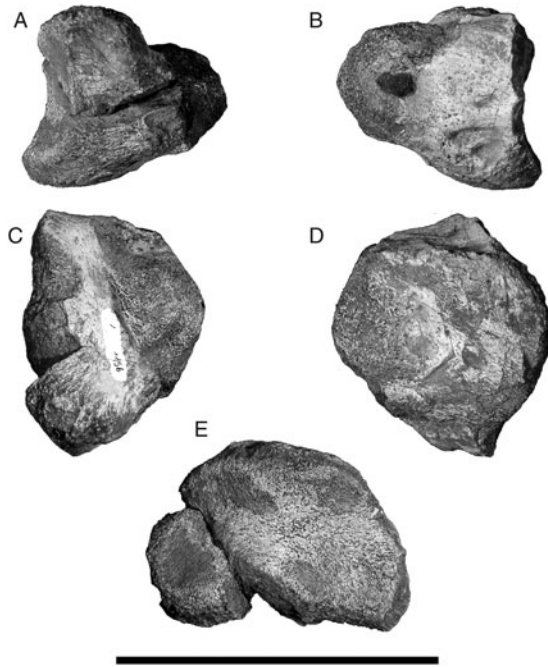


Figure 32. *Tyrannotitan chubutensis* phalange IV-3 (MPEF-PV 1157) photographs in (A) medial view, (B) lateral view, (C) ventral view, (D) dorsal view and (E) proximal view. Note: Scale bar is 10 cm; see text for abbreviations.

variation or it could represent a pathologic feature of the holotype. Although we consider further material is needed to determine the degree of variation of this character in *Tyrannotitan*, we have left for the moment this feature among the autapomorphies of *Tyrannotitan* following previous authors (Novas et al. 2005; Sereno and Brusatte 2008; Carrano et al. 2012), given that this condition has not been recorded in any other known theropod.

**6.1.1.2 Deep mental groove on the dentary.** The morphology, depth and orientation of the anterior end of the Meckelian groove in *Tyrannotitan* do not significantly differ from those of other theropod species, such as *Carcharodontosaurus iguidensis* (MNN IGU 5), *Giganotosaurus carolinii* (MUCPV-Ch 1) or *Allosaurus fragilis* (UMNH-VP 9351) (Appendix S1: Figure 1: A-B). Therefore, we have excluded this feature as an autapomorphy of *Tyrannotitan*, in contrast to previous proposals (Novas et al. 2005; Carrano et al. 2012).

**6.1.1.3 Posterior dorsal vertebrae with strongly developed ligament scars on neural spines.** In *Tyrannotitan*, the neural spines of the posterior dorsal vertebrae have well-developed ligament scars, ornamented with rounded and anterolaterally oriented projections. This character, originally noted in a preliminary study of *Tyrannotitan*

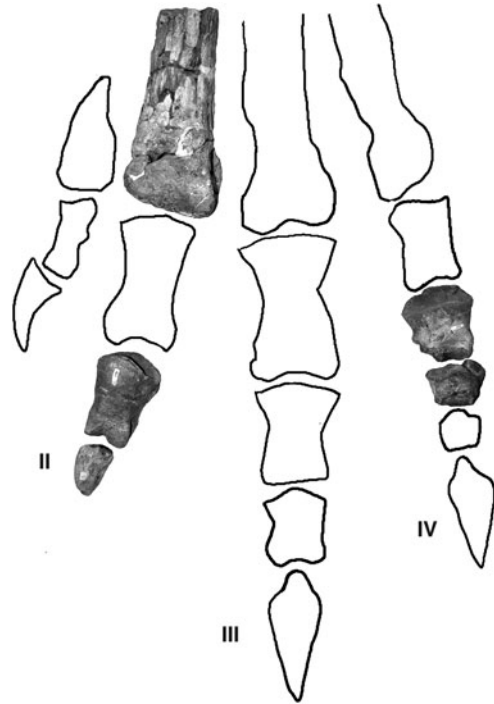


Figure 33. Reconstruction of the left foot of *Tyrannotitan chubutensis* based on elements of the paratype (MPEF-PV 1157).

(Rich et al. 2000), was considered as an autapomorphy of this genus by Novas et al. (2005). However, the same condition was described for *Acrocanthosaurus atokensis* (Harris 1998), and is present in *Mapusaurus roseae* (MCF-PVPH 108) and *Giganotosaurus carolinii* (MUCPV-Ch 1) (Appendix S1: Figure 1: C-D). In consequence, this character has been excluded from the emended diagnosis of *Tyrannotitan*.

#### 6.1.2 New autapomorphic characters of *Tyrannotitan*

Based on observations made in this study, four new characters were identified as autapomorphic features of *Tyrannotitan*.

**6.1.2.1 Symphyseal margin of dentary with anteroventral–posterodorsal inclination in lateral view.** Several allosauroids have a characteristic squared anterior end and subvertical symphyseal margin in the dentary (Sereno and Brusatte 2008). However, in *Tyrannotitan* the anteroventral corner of the symphyseal margin is slightly anterior to the anterodorsal corner, which gives a very slight anteroventral–posterodorsal inclination to this margin (Figure 34 (B)). This condition is absent in other theropods, including all known carcharodontosaurids (Brusatte and Sereno 2007; Sereno and Brusatte 2008), and is present in both the holotype and the paratype specimens of *Tyrannotitan*.

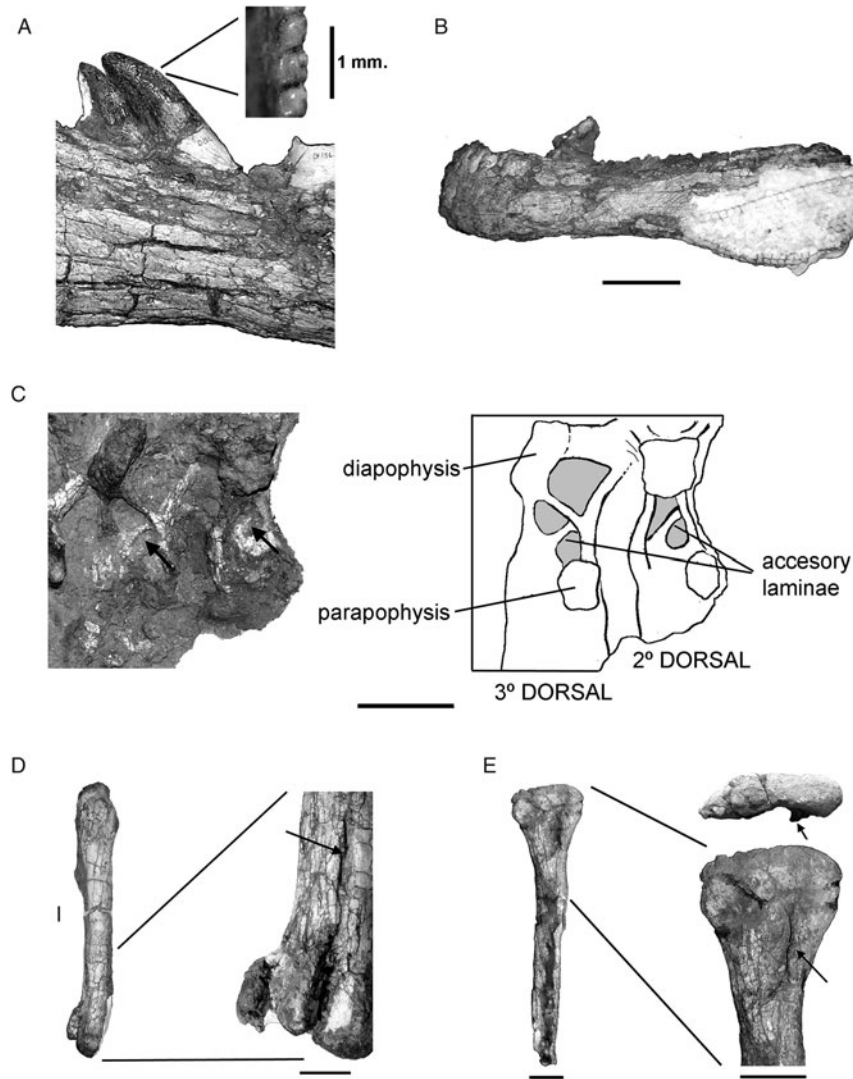


Figure 34. Autapomorphic characters of *Tyrannotitan chubutensis*. (A) detail photograph of the teeth with bilobated denticles, (B) photograph of the left dentary in lateral view, showing the vertical symphyseal margin, (C) photograph and line drawing of the second and third dorsal vertebrae in lateral view, showing the accessory laminae, (D) photograph of the right femur in medial view with a detail of the fibular fossa extended on the shaft and (E) photograph of the left fibula in medial view with a detail of the anterior border of the fibular fossa posteriorly projected. Note: Scale bar is 1 mm in (A) and 10 cm in (B)–(E).

**6.1.2.2 Second and third dorsal vertebrae with well-developed accessory laminae connecting anterior and posterior centrodiapophyseal laminae.** This character is also present in *Acrocanthosaurus atokensis* (Harris 1998), although in *Tyrannotitan* this is a very well-developed lamina. This character has been preserved only in the holotype, given that the paratype has not preserved these dorsal vertebrae (Figure 34(C)).

**6.1.2.3 Fibular fossa extended over the proximal end of the crista tibiofibularis in the femoral shaft.** In *Tyrannotitan* the fibular fossa is laterally delimited by the lateral tibial condyle and the crista tibiofibularis, as

occurring in most theropods. However, in *Tyrannotitan* this fossa extends proximally in the form of a groove that approaches the proximal margin of the tibiofibular crest in the femoral diaphysis (Figure 34(D)). This character is a unique feature of *Tyrannotitan*, and is present in both holotype and paratype.

**6.1.2.4 Proximomedial fossa of the fibula with posteriorly projected anterior border.** In *Tyrannotitan* the anterior edge of the proximomedial fossa is developed as a posteriorly oriented projection, covering part of the fossa in medial view (Figure 24(E)). In allosauroids, such as *Allosaurus* (UMNH-VP 6400), *Neovenator* (Brusatte et al.

2008), *Giganotosaurus* (MUCPV-Ch 1) and *Mapusaurus* (MCF-PVPH 108.202), this margin is smooth and lacks any type of projection or well-developed margin.

## 6.2 Remarks on carcharodontosaurid anatomy

### 6.2.1 Vertebral anatomy

The vertebral anatomy of carcharodontosaurids has not been fully analysed yet. For instance, the derived carcharodontosaurid *Giganotosaurus carolinii* (Coria and Salgado 1995) has preserved a complete vertebral series, but these remains are still undescribed in detail. The study of the vertebrae of *Tyrannotitan* revealed striking similarities with those of *Giganotosaurus*, *Carcharodontosaurus* and *Mapusaurus*, and to a lesser degree with the vertebrae of *Acrocanthosaurus*.

The cervical vertebrae in *Tyrannotitan* are strongly opisthocoelic, with the anterior articular face subspherical, as in *Giganotosaurus* (MUCPV-Ch 1) and *Carcharodontosaurus* (NCSM 18166). The neural spines are robust and 'pyramid-shaped' in anterior view, a feature that can also be seen in *Giganotosaurus* (MUCPV-Ch 1) and *Mapusaurus* (MCF-PVPH 108.90). The cervical centra have two pleurocoels on their lateral sides, as in *Giganotosaurus* (MUCPV-Ch 1), *Carcharodontosaurus* (NCSM 18166) and *Acrocanthosaurus* (Harris 1998). At least the posterior cervicals have rudimentary hyposphene–hypantrum accessory articulations, resembling the condition of *Giganotosaurus* (MUCPV-Ch 1) and *Carcharodontosaurus* (NCSM 18166). All the dorsal vertebrae also bear two pleurocoels on each side of the centrum (except for dorsal 14, which has a single pleurocoel) and the prezygapophyses have pneumatic openings or pits on their anterior borders as in *Mapusaurus* (MCF-PVPH 108.80) and *Giganotosaurus* (MUCPV-Ch 1). The neural spines are high, robust and rectangular in cross section, with strongly developed and prominent ligament scars and spinopre- and spinopostzygapophyseal fossae below them, as in *Acrocanthosaurus* (Harris 1998), *Mapusaurus* (MCF-PVPH 108.80) and *Giganotosaurus* (MUCPV-Ch 1). The sacrum is composed of five fused vertebrae, ventrally concave in lateral view, laterally compressed at its anteroposterior midpoint, and with unfused neural spines, as in *Giganotosaurus* (MUCPV-Ch 1). The posterior sacral centra have a single pleurocoel on each lateral side as in *Giganotosaurus* (MUCPV-Ch 1) and *Mapusaurus* (MCF-PVPH 108.209). Finally, the anterior caudal vertebrae only have pneumatic depressions (lacking true pleurocoels) on the lateral surfaces of their centra, as in *Giganotosaurus* (MUCPV-Ch 1) and *Mapusaurus* (MCF-PVPH 108.81).

The absence of pleurocoels in the first sacral centrum and the presence of pleurocoels in the last dorsals and in the fourth and fifth sacral vertebrae suggest the presence of a caudosacral pneumatic hiatus (Wedel 2009). A

pneumatic hiatus is an apneumatic portion of the vertebral column bracketed between pneumatic vertebrae, which has been interpreted as indicative of different air sacs or diverticula that pneumatise different parts of the skeleton. In the case of *Tyrannotitan*, the position of the hiatus suggest that different diverticula of the abdominal air sac pneumatized the last dorsals and the last sacral vertebrae independently. This interpretation is reinforced by the presence of only one pleurocoel in the posteriormost dorsal vertebra compared with the double opening of the preceding dorsal vertebrae, suggesting that the source of the presacral pneumatization is not completely expanded posteriorly. The presence of this hiatus has not been previously reported in theropods but has been described for the sauropod *Haplocantosaurus* (Wedel 2009). Its presence provides further evidence for inferring the development of abdominal air sacs with different diverticula, in addition to the cervical and clavicular air sacs in theropods, as occurring in birds (Wedel 2009).

### 6.2.2 Scapular girdle

The study of the scapulocoracoid in *Tyrannotitan* allows reinterpreting the morphology of this anatomical region in the closely related *Giganotosaurus* (Coria and Salgado 1995; Calvo 1999; Calvo et al. 2004; Novas et al. 2005; Novas 2009). In the original description, Coria and Salgado (1995) cited the following character as part of the diagnosis of *Giganotosaurus*: 'proximal end of the scapula forwardly projected over the coracoid'. In the description of the specimen they detailed that 'the coracoid is small and hook shaped with an externally open coracoid foramen'. This particular morphology was cited in subsequent contributions (Calvo 1999; Calvo et al. 2004; Novas et al. 2005) as a derived condition of *Giganotosaurus* that was absent in related forms.

A detailed comparison between the scapulocoracoid of *Tyrannotitan* and *Giganotosaurus* reveals that in the coracoid of the holotype of *Giganotosaurus*, the dorsal and anterior borders are damaged and only the sector over the glenoid cavity is preserved. The scapula of the type specimen of *Giganotosaurus* also has the acromial process broken, which was previously interpreted as a low acromial process (Calvo et al. 2004). The character 'externally open coracoid foramen' is also produced by a misinterpretation of the type material of this taxon. The coracoid foramen is present, but in a fragment of the left coracoid that is fused and preserved attached to the scapula (Figure 35(A)). This fragment of the coracoid was interpreted as part of the scapula by previous authors, but the suture scar between the coracoid and scapula is visible in the type material. The position of the coracoid foramen is almost the same as in *Tyrannotitan*, located centrally on the lateral surface of coracoid. The

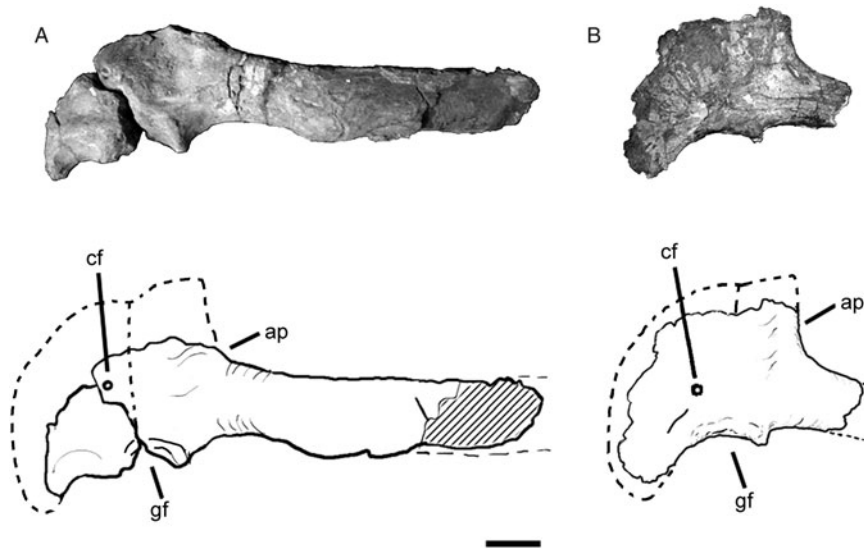


Figure 35. Scapulocoracoids in lateral view of (A) *Giganotosaurus carolinii* (MUCPV-Ch 1) and (B) *Tyrannotitan chubutensis* (MPEF-PV 1156). Note: Scale bar is 10 cm; see text for abbreviations.

interpretation of the fragment of the coracoid as part of the scapula led previous authors to postulate the autapomorphic character of *Giganotosaurus* ‘proximal end of the scapula forwardly projected over the coracoid’ (Coria and Salgado 1995) or, as expressed by Calvo et al. (2004), the ‘articular margin of the scapula–coracoid oblique with respect to the long axis of the scapula’.

In sum, the pectoral girdle of the type material of *Giganotosaurus* (Coria and Salgado 1995) is incompletely preserved and led to a misinterpretation of its anatomy. We interpret the scapula and coracoid of *Giganotosaurus* as similar to that of *Tyrannotitan* (Novas et al. 2005) and *Mapusaurus roseae* (Coria and Currie 2006), having a wide coracoid, well-developed coracoid foramen, scapula and coracoid fused, and the contact between these two elements is oriented perpendicular to the long axis of scapula. Although the acromion is only partially preserved in the holotype of *Giganotosaurus*, the available remains suggest its morphology did not differ from that of *Tyrannotitan*.

### 6.3 Phylogenetic analysis

The phylogenetic position of *Tyrannotitan chubutensis* within Carcharodontosauridae has been debated in recent phylogenetic analyses (Novas et al. 2005; Brusatte and Sereno 2008; Sereno and Brusatte 2008; Smith et al. 2008; Eddy and Clarke 2011). Previous analyses have retrieved *Tyrannotitan* as a basal carcharodontosaurid (Novas et al. 2005; Brusatte and Sereno 2008; Eddy and Clarke 2011) or in a polytomy with other derived carcharodontosaurids (Brusatte et al. 2008; Carrano et al. 2012). Probably this lack of agreement came from the limited anatomical

information available, given the lack of a detailed anatomical description of this taxon. The study of cranial and postcranial remains of *Tyrannotitan chubutensis* and comparisons with other carcharodontosaurids provided valuable information, which allows us testing more thoroughly their phylogenetic relationships.

The phylogenetic relationships of the clade Allosaurioidea, and in particular Carcharodontosauridae, have been the subject of intense research and debate, counting with more than 15 phylogenetic analyses published in recent years (Sereno et al. 1996; Harris 1998; Forster 1999; Currie and Carpenter 2000; Holtz 2000; Allain 2002; Coria and Currie 2002; Rauhut 2003; Holtz et al. 2004; Novas et al. 2005; Coria and Currie 2006; Smith et al. 2007; Brusatte and Sereno 2008; Sereno and Brusatte 2008; Smith et al. 2008; Brusatte et al. 2009; Benson 2010; Benson et al. 2010; Ortega et al. 2010; Eddy and Clarke 2011; Carrano et al. 2012; Cau et al. 2012a, 2012b; Novas et al. 2013). Here we present a phylogenetic analysis of Carcharodontosauridae based on the original data-set of Canale (2010), expanding the character sampling regime and changing some previous scorings (Table S1: Character re-scoring table). This data-set is an updated version of that presented in a recent review by Novas et al. (2013). The data matrix includes 16 taxa scored across 169 anatomical characters, 106 of which are cranial and 63 postcranial (Appendix S2: List of Anatomical Characters and S3: Data Matrix). The data matrix was analysed with TNT v1.1 (Goloboff et al. 2008). A heuristic search was carried out with 1000 replicates of Wagner trees (using random addition sequence) followed by tree bisection and reconnection (TBR) branch-swapping, saving 10 trees per replication, to find the most parsimonious trees (MPTs).

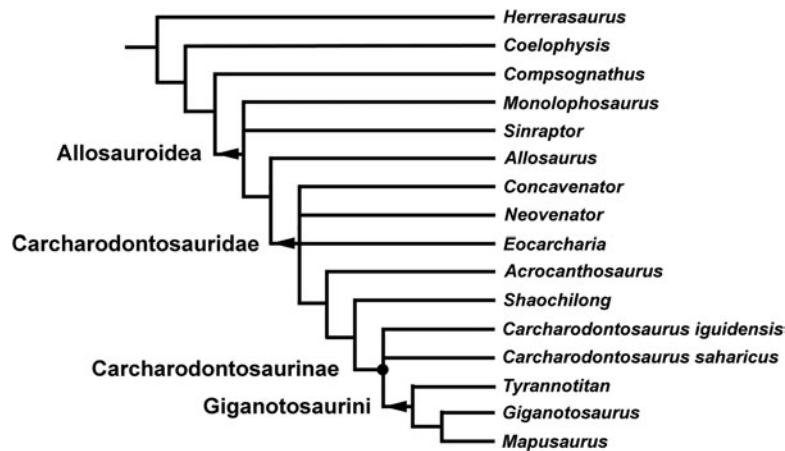


Figure 36. Strict consensus tree of the two MPTs obtained from the phylogenetic analysis.

A final round of TBR was applied to the best trees found in the replicates to ensure that all MPTs were found. Twelve MPTs of 308 steps were recovered (CI = 0.633; IR = 0.726).

### 6.3.1 Giganotosaurini

The strict consensus tree places *Tyrannotitan* in a derived position within Carcharodontosauridae, it being the sister group of *Giganotosaurus* and *Mapusaurus* (Figure 36). These three taxa form the clade Giganotosaurini, as also noted by Novas et al. (2013). In this phylogenetic analysis, the clade Giganotosaurini is diagnosed by three two unambiguous synapomorphies.

The first of these is the presence of a postorbital process of the jugal with a wide base (char. 60:0), a character recently recognised by Novas et al. (2013). In *Allosaurus* (UMNH-VP 9085), *Monolophosaurus* (Zhao and Currie 1993), *Sinraptor* (Currie and Zhao 1993), *Acrocanthosaurus* (NCSM 14345) and *Carcharodontosaurus saharicus* (SGM-Din1), the postorbital process of the jugal is rod-like, its height being equal or more than twice the anteroposterior length of its base. In *Mapusaurus* (MCF-PVPH 108.168) and *Tyrannotitan* (MPEF-PV 1157), the postorbital process of jugal is subtriangular in lateral view, its height being less than twice the length of its base (Figure 37).

The second synapomorphy of Giganotosaurini is the presence of a shallow and broad extensor groove on distal femur (char. 161:1). This character was originally proposed by Harris (1998) and later Coria and Currie (2006) considered state 1 as a synapomorphy that unites *Giganotosaurus* and *Mapusaurus*. A shallow and broad extensor groove is also present in *Tyrannotitan* (MPEF-PV 1156) (Appendix S1: Figure 2).

The clade Giganotosaurini has minimal Bremer support values (BS = 1); however, this is mainly due to the unstable behaviour of *Carcharodontosaurus iguidensis* in suboptimal trees. When the alternative positions of the highly incomplete *Carcharodontosaurus iguidensis* (76% missing data) are ignored among the suboptimal trees, the

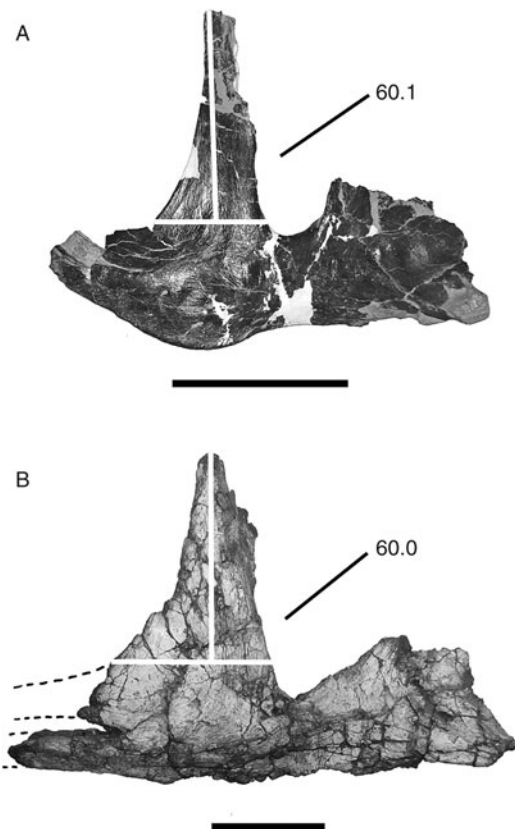


Figure 37. Illustration of character 60. Right jugals of (A) *Allosaurus fragilis* (UMNH-VP 9085) and (B) *Tyrannotitan chubutensis* (MPEF-PV 1157). Note: Scale bar is 10 cm.

monophyly of the clade Giganotosaurini is only rejected in trees that are three steps longer than the MPTs (BS = 3). This demonstrates that despite the uncertainties on the phylogenetic position of *Carcharodontosaurus iguidensis* due to its fragmentary nature, the clustering of the three South American taxa (*Tyrannotitan*, *Mapusaurus* and *Giganotosaurus*) to the exclusion of *Carcharodontosaurus saharicus* and other carcharodontosaurids is moderately well supported.

*Tyrannotitan* is placed basally within Giganotosaurini (Figure 36) because it lacks two derived features present in the femur of *Mapusaurus* and *Giganotosaurus*, which are interpreted in the context of this analysis as unambiguous synapomorphies of the clade formed by these two taxa. These are the strongly reduced fourth trochanter on femur (char. 160:1) and the absence of the ridge for cruciate ligaments in flexor groove of femur (char. 162:0).

### 6.3.2 *Carcharodontosaurinae*

Giganotosaurini and the African genus *Carcharodontosaurus* are retrieved as sister taxa (Figure 36), forming the clade Carcharodontosaurinae: a group of giant-sized, derived, gondwanan carcharodontosaurids. The monophyly of this clade is supported by the four cranial characters proposed in previous studies that are interpreted here as unambiguous synapomorphies: the maxilla with only promaxillary foramen on the antorbital fossa (char. 7:3), external sculpturing of maxilla covering the main body of the bone (char. 13:1), strong rugosities and projections over the anterior half of the nasal (char. 25:1) and interorbital septum present and well ossified (char. 77:1). It is worth noting that the condition of *Tyrannotitan* for these four cranial synapomorphies is unknown. However, the support for the inclusion of this taxon deeply nested within Carcharodontosaurinae comes from the derived features shared with *Mapusaurus* and *Giganotosaurus* noted above (see Giganotosaurini; chars. 60, 161).

The support value for Caracharodontosaurinae is higher than that for the clade Giganotosaurini within the context of the analysed data matrix. In trees that are three to seven steps longer than the most parsimonious topology, both *Shaochilong* and *Eocarcharia* get nested within this clade, but not other carcharodontosaurid taxa. This indicates that despite the uncertainties on the position of *Shaochilong* and *Eocarcharia* (both of which are fragmentary and with large amounts of missing data in this data-set), the clade Carcharodontosaurinae has strong character support within Carcharodontosauridae.

The monophyly of this Gondwanan clade of giant theropods and its internal divergence between the clades *Carcharodontosaurus* (recorded in the Cenomanian of northern Africa) and Giganotosaurini (recorded from the

Albian to the Cenomanian in southern South America) are compatible with a vicariant explanation of their distribution, given that the separation between both continents was apparently effective at some point during the Aptian–Albian (Gheerbrant and Rage 2006).

### 6.3.3 *Carcharodontosauridae*

The monophyly of Carcharodontosauridae is supported by 18 synapomorphies: maxilla with fully co-ossified posterior interdental plates (char. 14:1), squared anterior margin of maxillary antorbital fossa (char. 20:1), maxilla with sinuous shape of ridge across interdental plates in medial view (char. 22:1), nasals parallel sided throughout its length in dorsal view (26:1), frontals co-ossified (char. 35:1), frontals co-ossified with parietal (char. 36:1), paired frontals mediolaterally wider than 4/3 of frontal length (char. 37:2), lacrimal and postorbital in contact (char. 41:1), transversely broad interlocking suture between postorbital and squamosal (char. 42:1), postorbital with suborbital flange (char. 43:1), postorbital with bulbous swelling extensively overhanging the orbit (char. 46:1), postorbital with vascular groove present and limited to anterior half of dorsal boss (char. 49:1), postorbital with expansion of supratemporal fossa close to posterior margin of main body in dorsal view (char. 50:1), large axial epiphyses (char. 109:1), cervicals with interior structure of centrum camellate (char. 118:2), dorsal vertebrae with hyposphene laminae parallel and sheet like (char. 122:1), ischium with a boot-shaped distal expansion (absent in more derived forms) (154:2) and tibial lateral malleolus distal extension beyond medial malleolus more than 5% tibial length (char. 167:1).

## 7. Conclusions

The carcharodontosaurid theropod *Tyrannotitan chubutensis* is here described improving our knowledge of the anatomy, the phylogenetic position of this taxon and the internal relationships of carcharodontosaurid dinosaurs. The original diagnosis of the species was revised and emended with four new autapomorphic characters. The available material of *Tyrannotitan* has provided new information on the axial skeleton, allowing a comparison with related forms on vertebral anatomy. The presence of a pneumatic hiatus in the sacrum of *Tyrannotitan* adds evidence to the presence of abdominal air sacs; with different diverticula pneumatizing different parts of the skeleton, in addition to the cervical and clavicular air sacs, as occurring in birds. *Tyrannotitan* shares several derived characters with *Giganotosaurus* and *Mapusaurus*, and to a lesser degree, with *Carcharodontosaurus* (for which there is limited vertebral information) and *Acrocanthosaurus*. The analysis of the pectoral girdle of *Tyrannotitan* allowed

a reinterpretation of the scapula and coracoid anatomy of the related carcharodontosaurid *Giganotosaurus*. Features of the latter genus previously interpreted as a derived morphology actually respond to misinterpretations of broken surfaces. The new anatomical information on *Tyrannotitan* and related forms was incorporated in a phylogenetic analysis that reinforces the hypothesis of *Tyrannotitan* being a derived carcharodontosaurid. In our results, this taxon is depicted as the sister group of *Giganotosaurus* plus *Mapusaurus*, forming the South American clade Giganotosaurini. The close affinities of *Tyrannotitan* with other South America forms and the position of the African *Carcharodontosaurus* as their sister group are concordant with previous hypotheses on the vicariant pattern of southern dinosaurs that resulted from the break up of Gondwana during the Cretaceous.

### Acknowledgements

The authors would like to thank Eduardo Ruigómez (MEF), Rodolfo Coria (MCF), Jorge Calvo (MUC), Alejandro Kramarz (MACN), Mike Getty (UMNH), Vince Schneider (NCSM), Paul Sereno (University of Chicago, USA), Rodney Scheetz (BYU) for allowing access to specimens under their care. Federico Agnolín made comments on early drafts of the manuscript. We also thank Andrea Cau (Museo Geologico 'Giovanni Capellini', Bologna, Italy) and an anonymous reviewer for their improving and useful comments on the manuscript, especially Dr Cau for his suggestions about axial pneumaticity. Miguel O. Manceñido helped with taxonomic and nomenclatural aspects.

### Funding

Travel finance to carry out this work was provided by the Jurassic Foundation (to JIC). The program TNT is made freely available, thanks to a subsidy by the Willi Hennig Society.

### Notes

1. Email: [fernovas@yahoo.com.ar](mailto:fernovas@yahoo.com.ar)
2. Email: [dpol@mef.org.ar](mailto:dpol@mef.org.ar)

### References

- Allain R. 2002. Discovery of megalosaur (Dinosauria, Theropoda) in the Middle Bathonian of Normandy (France) and its implications for the phylogeny of basal Tetanurae. *J Vert Paleontol.* 22(3):548–563.
- Apesteguía S, Carballido JL. in press. A new eilenodontine (Lepidosauria, Sphenodontidae) from the Lower Cretaceous of central Patagonia. *J Vert Paleontol.*
- Argarñaz E, Grellet-Tinner G, Fiorelli LE, Krause M, Rauhut OWM. 2013. Huevos de saurópodos del Aptiano-Albiano, Formación Cerro Barco (Patagonia, Argentina): un enigma paleoambiental y paleobiológico. *Ameghiniana.* 50(1):33–50.
- Benson RBJ. 2010. A description of *Megalosaurus bucklandii* (Dinosauria: Theropoda) from the Bathonian of the UK and the relationships of Middle Jurassic theropods. *Zool J Linn Soc.* 158:882–935.
- Benson RBJ, Brusatte SL, Carrano MT. 2010. A new clade of archaic large-bodied predatory dinosaurs (Theropoda: Allosauroida) that survived to the latest Mesozoic. *Naturwissenschaften.* 97:71–78.
- Bonaparte JF. 1986. Les dinosaurios (Carnosures, Allosauridés, Sauropodes, Cetiosauridés) du Jurassique Moyen de Cerro Cóndor (Chubut, Argentine). *Ann Paleontol.* 72:247–289.
- Brochu CA. 2003. Osteology of *Tyrannosaurus rex*: insights from a nearly complete skeleton and high-resolution computer tomographic analysis of the skull. *J Vert Paleontol Mem.* 7:1–140.
- Brusatte SL, Benson RBJ, Carr TD, Williamson TE, Sereno PC. 2007. The systematic utility of theropod enamel wrinkles. *J Vert Paleontol.* 27(4):1052–1056.
- Brusatte SL, Benson RBJ, Chure DJ, Xu X, Sullivan C, Hone DWE. 2009. The first definitive carcharodontosaurid (Dinosauria: Theropoda) from Asia and the delayed ascent of tyrannosaurids. *Naturwissenschaften.* 96:1051–1058.
- Brusatte SL, Benson RBJ, Hutt S. 2008. The osteology of *Neovenator salerii* (Dinosauria: Theropoda) from the Wealden Group (Barremian) of the Isle of Wight. *Monograph Palaeontograph Soc.* 162(631):1–166.
- Brusatte SL, Benson RBJ, Xu X. 2012. A reassessment of *Kelmaysaurus petroliticus*, a large theropod dinosaur from the Early Cretaceous of China. *Acta Palaeontol Pol.* 57(1):65–72.
- Brusatte SL, Sereno PC. 2007. A new species of *Carcharodontosaurus* (Dinosauria: Theropoda) from the Cenomanian of Niger and a revision of the genus. *J Vert Paleontol.* 27(4):902–916.
- Brusatte SL, Sereno PC. 2008. Phylogeny of Allosauroida (Dinosauria: Theropoda): comparative analysis and resolution. *J Syst Paleontol.* 6:155–182.
- Canale JJ. 2010. Los Carcharodontosauridae (Dinosauria, Theropoda) del Cretácico de América del Sur: anatomía, relaciones filogenéticas y paleobiología. Unpublished PhD Thesis. Facultad de Ciencias Naturales y Museo, Universidad Nacional de La Plata, 261 pp.
- Canale JJ, Scanferla CA, Agnolín FL, Novas FE. 2009. New carnivorous dinosaur from the Late Cretaceous of NW Patagonia and the evolution of abelisauroid theropods. *Naturwissenschaften.* 96:409–414.
- Calvo JO. 1999. Dinosaurs and other vertebrates of the Lake Ezequiel Ramos Mexía Area, Neuquén-Patagonia, Argentina. In: Tomida Y, Rich TH, Vickers-Rich P, editors. *Proceedings of the 2nd Gondwanan dinosaur symposium.* *Nat Sci Mus Monographs, Tokyo.* vol. 15. p. 13–45.
- Calvo JO, Porfiri J, Veralli C, Novas FE, Poblete F. 2004. Phylogenetic status of *Megaraptor namunhuaiquii* Novas based on a new specimen from Neuquén, Patagonia, Argentina. *Ameghiniana.* 41(4):565–575.
- Carballido JL, Pol D, Cerda I, Salgado L. 2011. The Osteology of *Chubutisaurus insignis* Del Corro, 1975 (Dinosauria: Neosauropoda) from the 'Middle' Cretaceous of Central Patagonia, Argentina. *J Vert Paleontol.* 31(1):93–110.
- Carrano MT, Benson RBJ, Sampson SD. 2012. The phylogeny of Tetanurae. *J Syst Paleontol.* 10(2):211–300.
- Cau A, Dalla Vecchia F, Fabbri M. 2012a. Evidence of a new carcharodontosaurid from the Upper Cretaceous of Morocco. *Acta Paleontol Pol.* 57(3):661–665.
- Cau A, Dalla Vecchia F, Fabbri M. 2012b. A thick-skulled theropod (Dinosauria, Saurischia) from the Upper Cretaceous of Morocco with implications for carcharodontosaurid cranial evolution. *Cretaceous Res.* 40:251–260.
- Codignotto J, Nullo F, Panza J, Proserpio C. 1978. Estratigrafía del Grupo Chubut entre Paso de Indios y Las Plumas, Provincia del Chubut, Argentina. *Actas VII Congreso Geológico Argentino.* 471–480.
- Coria RA, Currie PJ. 2002. The braincase of *Giganotosaurus carolinii* (Dinosauria: Theropoda) from the Upper Cretaceous of Argentina. *J Vert Paleontol.* 22(4):802–811.
- Coria RA, Currie PJ. 2006. A new carcharodontosaurid (Dinosauria, Theropoda) from the Upper Cretaceous of Argentina. *Geodiversitas.* 28(1):71–118.
- Coria RA, Salgado L. 1995. A new giant carnivorous dinosaur from the Cretaceous of Patagonia. *Nature.* 377:224–226.
- Currie PJ, Carpenter K. 2000. A new specimen of *Acrocanthosaurus atokensis* (Theropoda, Dinosauria) from the Lower Cretaceous Antlers Formation (Lower Cretaceous, Aptian) of Oklahoma, USA. *Geodiversitas.* 22:207–246.

- Currie PJ, Rigby JK. Jr, Sloan RE. 1990. Dinosaur systematics: perspectives and approaches. In: Carpenter K, Currie PJ, editors. Theropod teeth from the Judith River Formation of southern Alberta, Canada. Cambridge: Cambridge University Press. p. 107–125.
- Currie PJ, Zhao X. 1993. A new carnosaur (Dinosauria, Theropoda) from the Jurassic of Xinjiang, People's Republic of China. *Can J Earth Sci.* 30:2037–2081.
- de la Fuente MS, Umazano AM, Sterli J, Carballido JL. 2011. New chelid turtles of the lower section of the Cerro Barcino Formation (Aptian-Albian?), Patagonia, Argentina. *Cretaceous Res.* 32:527–537.
- Del Corro G. 1975. Un nuevo saurópodo del Cretácico Superior, *Chubutisaurus insignis* (Saurischia-Chubutisauridae), Chubut, Argentina. *Actas I Congr Argentino Paleontol Bioestratigr.* 2:229–240.
- Eddy D, Clarke J. 2011. New information on the cranial anatomy of *Acrocanthosaurus atokensis* and its implications for the phylogeny of Allosauroidea (Dinosauria: Theropoda). *PLoS ONE.* 6:e17932.
- Fanti F, Therrien F. 2007. Theropod tooth assemblages from the Late Cretaceous Maevarano Formation and the possible presence of dromaeosaurids in Madagascar. *Acta Paleontol Pol.* 52(1):155–166.
- Forster CA. 1999. Gondwanan dinosaur evolution and biogeographic analysis. *J African Earth Sci.* 28:169–185.
- Gaffney ES, Rich TH, Vickers-Rich P, Constantine A, Vacca R, Kool L. 2007. *Chubutemys*, a new Eucryptodiran turtle from the Early Cretaceous of Argentina, and the relationships of the Meiolaniidae. *Am Mus Novitates.* 3599:1–35.
- Gheerbrant E, Rage J-C. 2006. Paleobiogeography of Africa: how distinct from Gondwana and Laurasia? *Palaeogeogr Palaeoclimatol Palaeoecol.* 241:224–246.
- Gilmore CW. 1920. Osteology of the carnivorous Dinosauria in the United States National Museum, with special reference to the genera *Antrodemus* (Allosaurus) and *Ceratosaurus*. *Bull United States Nat Mus.* 110:1–159.
- Goloboff PA, Farris S, Nixon A. 2008. TNT, a free program for phylogenetic analysis. *Cladistics.* 24(5):774–786.
- Harris JD. 1998. A reanalysis of *Acrocanthosaurus atokensis*, its phylogenetic status and paleobiogeographic implications, based on a new specimen from Texas. *Bull New Mexico Mus Nat Hist Sci.* 13:1–75.
- Holliday CM. 2009. New insights into dinosaur jaw muscle anatomy. *Anat Rec.* 292:1246–1265.
- Holtz TR. 2000. A new phylogeny of the carnivorous dinosaurs. *GAIA.* 15:5–61.
- Holtz TR, Molnar RE, Currie PJ. 2004. The Dinosauria. In: Weishampel D, Dodson P, Osmólska H, editors. *Basal Tetanurae*. 2nd ed.. Berkeley, CA: California University Press. p. 343–362.
- Leardi JM, Pol D. 2009. The first crocodyliform from the Chubut Group (Chubut Province, Argentina) and its phylogenetic position within basal Mesoeucrocodylia. *Cretaceous Res.* 30(6):1376–1386.
- Madsen JH. 1976. *Allosaurus fragilis*: a revised osteology. *Utah Geol Mineral Surv Bull.* 109:3–163.
- Marveggio N, Llorens M. 2013. Nueva edad de la base del Grupo Chubut en la mena uranífera Cerro Solo, Provincia de Chubut. *Rev Asoc Geol Argentina.* 70(3):318–326.
- Musacchio E, Chebli W. 1975. Ostrácodos no marinos y carófitas del Cretácico inferior de las provincias de Chubut y Neuquén, Argentina. *Ameghiniana.* 12:70–96.
- Novas FE. 2009. The Age of Dinosaurs in South America. Indiana: Indiana University Press. p. 1–536.
- Novas FE, Agnolín FL, Ezcurra MD, Porfiri J, Canale JI. 2013. Evolution of the carnivorous dinosaur during the Cretaceous: the evidence from Patagonia. *Cretaceous Res.* 1–42. <http://dx.doi.org/10.1016/j.cretres.2013.04.001>
- Novas FE, Bandyopadhyay S. 2001. Abelisaurid pedal unguals from the Late Cretaceous of India. In: VIIIth international symposium on Mesozoic terrestrial ecosystems. vol. 7 Asociación Paleontológica Argentina, Publicación Especial. p. 145–149.
- Novas FE, de Valais S, Vickers Rich P, Rich T. 2005. A large Cretaceous theropod from Patagonia, Argentina, and the evolution of carcharodontosaurids. *Naturwissenschaften.* 92:226–230.
- O'Connor P. 2007. The postcranial axial skeleton of *Majungasaurus crenatissimus* (Theropoda: Abelisauridae) from the late Cretaceous of Madagascar. *J Vert Paleontol.* 27(2):127–172.
- Ortega F, Escaso F, Sanz JL. 2010. A bizarre, humped Carcharodontosauria (Theropoda) from the Lower Cretaceous of Spain. *Nature.* 467:203–206.
- Page R, Ardolino A, de Barrio RE, Franchi M, Lizuain A, Page S, Silva Nieto D. 1999. Geología Argentina. In: Caminos R, editor. *Estratigrafía del Jurásico y Cretácico del Macizo de Somún Curá, Provincias de Río Negro y Chubut*. Buenos Aires: Subsecretaría de Minería de la Nación. p. 460–488.
- Rauhut OWM. 1995. Zur systematischen Stellung der afrikanischen Theropoden *Carcharodontosaurus* Stromer 1931 und *Bahariasaurus* Stromer 1934. *Berl Geowiss Abhandl.* 16(1):357–375.
- Rauhut OWM. 2003. The interrelationships and evolution of basal theropod dinosaurs. *Special Papers in Palaeontology* no. 69. London, 213 pp. Paleontological Association.
- Rauhut OWM. 2004. Provenance and anatomy of *Genyodectes serus*, a large-toothed ceratosaur (Dinosauria: Theropoda) from Patagonia. *J Vert Paleontol.* 24(4):894–902.
- Rauhut OWM. 2011. Theropod dinosaurs from the Late Jurassic of Tendaguru (Tanzania). *Special Papers in Palaeontology.* 86:195–239.
- Rauhut OWM, Cladera G, Vickers-Rich P, Rich TH. 2003. Dinosaur remains from the Lower Cretaceous of the Chubut Group, Argentina. *Cretaceous Res.* 24:487–497.
- Rich TH, Vickers-Rich P, Novas F, Cúneo R, Puerta P, Vacca R. 2000. Theropods from the 'Middle' Cretaceous Chubut Group of the San Jorge sedimentary basin, Central Patagonia. A preliminary note. *GAIA.* 15:111–115.
- Sereno PC, Brusatte SL. 2008. Basal abelisaurid and carcharodontosaurid theropods from the Lower Cretaceous Elrhaz Formation of Niger. *Acta Paleontol Pol.* 53(1):15–46.
- Sereno PC, Dutheil DB, Iarochene M, Larsson HC, Lyon GH, Magwene PM, Sidor CA, Varrichio DJ, Wilson JA. 1996. Predatory dinosaurs from the Sahara and Late Cretaceous faunal differentiation. *Science.* 272:986–991.
- Sereno PC, Martínez RN, Wilson JA, Varrichio DJ, Alcober OA, Larsson HCE. 2008. Evidence for avian intrathoracic air sacs in a new predatory dinosaur from Argentina. *PLoS ONE.* 3(9):e3303.
- Sereno PC, Wilson JA, Conrad JL. 2004. New dinosaurs link southern landmasses in the Mid-Cretaceous. *Proc B R Soc Lond.* 271:1325–1330.
- Smith ND, Makovicky PJ, Agnolín FL, Ezcurra MD, Pais DF, Salisbury SW. 2008. A Megaraptor-like theropod (Dinosauria: Tetanurae) in Australia: support for faunal exchange across eastern and western Gondwana in the mid-Cretaceous. *Proc B R Soc Lond.* 275:1647–2085.
- Smith ND, Makovicky PJ, Hammer WR, Currie PJ. 2007. Osteology of *Cryolophosaurus ellioti* (Dinosauria: Theropoda) from the Early Jurassic of Antarctica and implications for early theropod evolution. *Zool J Linn Soc.* 151:377–421.
- Sterli J, de la Fuente MS, Umazano AM. 2013. New remains and new insights on the Gondwanan meiolaniform turtle *Chubutemys copelloi* from the Lower Cretaceous of Patagonia, Argentina. *Gondwana Res.* <http://dx.doi.org/10.1016/j.gr.2013.08.016>
- Stromer E. 1931. Wilbeltierreste der Baharije-Stufe (unterstes Cenoman). 10. Ein Skelett-Rest von *Carcharodontosaurus* nov. gen. *Abhandlungen der Königlich Bayerischen Akademie der Wissenschaften, Mathematisch-Naturwissenschaftliche Abteilung.* Neue Folge. 9:1–23.
- Wedel MJ. 2009. Evidence for bird-like air sacs in Saurischian dinosaurs. *J Exp Zool.* 311A:611–628.
- Wilson JA, D'Emic MD, Ikejiri T, Moacdieh EM, Whitlock JA. 2011. A nomenclature for vertebral fossae in sauropods and other saurischian dinosaurs. *PLoS ONE.* 6(2):e17114.
- Zhao X, Currie PJ. 1993. A large crested theropod from the Jurassic of Xinjiang, People's Republic of China. *Can J Earth Sci.* 30:2027–2036.